JOURNAL OF MOLECULAR SPECTROSCOPY 53, 150–188 (1974)

Calculated Vibrational Transition Probabilities of OH($X^2\Pi$)

FREDERICK H. MIES

National Bureau of Standards, Washington, D.C. 20234

The theoretically derived dipole moment function of OH($X^2\Pi$) obtained by Stevens Das, Wahl, Neumann, and Krauss is used to calculate the absolute intensities of the vibrational–rotational transitions of the OH Meinel bands. The calculations take full account of the spin uncoupling and vibration–rotation coupling which markedly influence the radiative transition probabilities. The effect of lambda-doubling on the vibrational transitions is analyzed and generally found to be negligible. Results are tabulated for $\Delta v = v' - v''$ ranging from the fundamental transitions $\Delta v = 1$ to the $\Delta v = 5$ overtone, for $v' = 1$–9 and $J' = 0.5$–15.5. A comparison is made with available data, and various features of the OH spectrum are examined that are of aeronomical and experimental interest. Thermally averaged emission rates are presented for $\Delta v = 1$–5, and the validity of the rotational temperatures commonly derived from experimental intensity distributions is questioned.

I. INTRODUCTION

The reaction of H with O_3 produces OH($X^2\Pi$) with vibrational excitation as high as $v' = 9$ (*1*). Subsequent emission spectra are observed with $\Delta v = v' - v''$ as high as 7. Many such overtone emissions of OH are observed in atmospheric twilight and night glow (*2, 3, 4*) and have come to be called the Meinel bands of OH. Similar emission is observed in laboratory reactions (*5, 6*), and the 3–1 and 2–0 transitions appear to exhibit stimulated emission under appropriate conditions (*7, 8*). Rotational temperatures derived from the Meinel band intensity distributions are widely used to characterize atmospheric conditions (*4, 9*). These variegated uses of the OH spectra suggest the need for a thorough analysis and accurate theoretical determination of the absolute intensities of the OH transitions.

A very accurate dipole moment function $d(R)$ has recently been calculated for OH($X^2\Pi$) by Stevens *et al.* (*10*) using MCSCF electronic wavefunctions. The R-dependence of the theoretical $d(R)$, which is shown in Fig. 1, substantiates the qualitative behavior of the rather uncertain dipole moment function derived from an assorted collection of experimental data (*11, 12*) and confirms the observation that the OH overtone intensities are large. The function is relatively flat in the region of R_e (which would lead to weak fundamental intensities at small v'), peaks at $R = 1.2$ Å, and falls-off exponentially at large R. This behavior is caused by a transfer of charge from the hydrogen to the oxygen in the region of overlap. Obviously, a truncated power series expansion of such a moment function, as is generally employed in the analysis of vibrational band intensities (*11, 12*), is poorly convergent and may produce highly misleading estimates of the transition probabilities for those transitions not included in the analysis.

A proper numerical integration over the exact dipole moment function, using accurate vibrational wavefunctions, is required.

Using the theoretically determined $d(R)$, we have calculated the absolute intensities of the OH vibration–rotation transitions utilizing numerically determined vibrational wavefunctions obtained from a composite of RKR (*13*), and theoretical (*10*) potentials. The calculations take full and accurate account of the spin-uncoupling effects and vibrational–rotational coupling effects on the total wavefunction for the $^2\Pi$ state. These effects are extremely large in OH, and will be analyzed in a subsequent paper (*14*) to test the validity of Hill and VanVleck's (HVV) theory of intermediate spin coupling (*15*) and the Herman and Wallis theory of vibrational–rotational coupling (*16*).

The resultant data are voluminous since the intensities are not easily factorable into the usual product of a rotational line strength and a vibrational band strength. The specific rotation–vibration transition probabilities for $\Delta v = 1, 2, 3, 4$ and 5 are given in this paper, and a tabulation of satellite band intensities will be made available (*17*). Thermally averaged band intensities are also presented, and specific features of the calculated intensities are discussed which relate to atmospheric studies and low resolution laboratory experiments.

II. CONSTRUCTION OF WAVEFUNCTION AND COUPLED RADIAL EQUATIONS

For a given total angular momentum state J, with space-fixed momentum projection M, and a given total parity $P = \pm 1$, the ground state of OH, in the vicinity of $R = R_e$ at least, is almost a pure $^2\Pi$ state, with a small admixture of the neighboring $^2\Sigma^+$ state due to spin–orbit and Λ-doubling effects.[1] The total electronic–rotational–vibrational wavefunction of the OH($X^2\Pi$) in its most general form is represented as follows.

$$|J, M, P\rangle = F_{\frac{1}{2}}(R)|J, M, P; {}^2\Pi_{\frac{1}{2}}\rangle + F_{\frac{3}{2}}(R)|J, M, P; {}^2\Pi_{\frac{3}{2}}\rangle + G^+(R)|J, M, P; {}^2\Sigma_{\frac{1}{2}}{}^+\rangle. \quad (1)$$

The individual electronic–rotational functions in Eq. (1) are eigenfunctions of the total angular momentum $\mathbf{J}^2$, and J_Z, and the total inversion operator, or parity operator I. They have been constructed in pure Hund's case (a) from the corresponding Born–Oppenheimer electronic wavefunctions for the ground $^2\Pi$ state, $|{}^2\Pi; \Lambda, \Sigma\rangle$, which has an electron orbital angular momentum projection $\Lambda = \pm 1$ along the molecular axis, and an electron spin projection $\Sigma = \pm \frac{1}{2}$, and the lowest $^2\Sigma^+$ state, $|{}^2\Sigma^+; 0, \Sigma\rangle$, with $\Lambda = 0$ and spin projection $\Sigma = \pm \frac{1}{2}$. The "quantum number" $\Omega = |\Lambda + \Sigma|$ is the magnitude of the total electron angular momentum projection along the molecular axis and takes the values $\frac{1}{2}$ and $\frac{3}{2}$ for the $^2\Pi$ state, and $\frac{1}{2}$ for the $^2\Sigma^+$ state. The effect of spin-uncoupling is, of course, to uncouple the electron spin projection from the molecular axis, thereby causing a mixing of the $^2\Pi_{\frac{1}{2}}$ and $^2\Pi_{\frac{3}{2}}$ states, while Λ-doubling uncouples the electron orbital angular momentum from the molecular axis causing a mixing of the Π and Σ states.

$$|J, M, P; {}^2\Pi_\Omega\rangle = 2^{-\frac{1}{2}}[\Omega_\Omega{}^{J,M}|{}^2\Pi; 1, \Omega - 1\rangle + Pe^{i\pi(J-\frac{1}{2})}\Omega_{-\Omega}{}^{J,M}|{}^2\Pi; -1, -\Omega + 1\rangle], \quad (2)$$

$$|J, M, P; {}^2\Sigma_{\frac{1}{2}}{}^+\rangle = 2^{-\frac{1}{2}}[\Omega_{\frac{1}{2}}{}^{J,M}|{}^2\Sigma^+; 0, \tfrac{1}{2}\rangle + Pe^{i\pi(J-\frac{1}{2})}\Omega_{-\frac{1}{2}}{}^{J,M}|{}^2\Sigma^+; 0, -\tfrac{1}{2}\rangle]. \quad (3)$$

[1] At large R significant mixing must occur with the $^4\Pi$ and $^{2,4}\Sigma^-$ states to effect adiabatic dissociation into H(^{2}S) plus O(^{3}P) in its proper asymptotic multiplet states.

The functions $\Omega_\Omega{}^{J,M}$ are normalized symmetric top wavefunctions which are defined in terms of the Wigner rotation matrices (*18*) and are dependent on the polar coordinates, θ and Φ, of the molecular axis,

$$\Omega_\Omega{}^{J,M}(\theta,\Phi) = [(2J+1)/4\pi]^{\frac{1}{2}} D_{M,\Omega}{}^{J*}(\Phi,\theta,0). \tag{4}$$

For a given J and M, Eqs. (2) and (3) define six states; however states of opposite parity do not interact[2] since the total Hamiltonian H, commutes with the inversion operator I, and Eq. (1) will generate a set of three coupled differential equations for the radial functions $F(R)$ and $G^+(R)$.

$$\langle {}^2\Pi_{\frac{1}{2}}|H-E|{}^2\Pi_{\frac{1}{2}}\rangle F_{\frac{1}{2}}(R) + \langle {}^2\Pi_{\frac{1}{2}}|H|{}^2\Pi_{\frac{3}{2}}\rangle F_{\frac{3}{2}}(R) = -\langle {}^2\Pi_{\frac{1}{2}}|H|{}^2\Sigma_{\frac{1}{2}}{}^+\rangle G^+(R), \tag{5}$$

$$\langle {}^2\Pi_{\frac{3}{2}}|H-E|{}^2\Pi_{\frac{3}{2}}\rangle F_{\frac{3}{2}}(R) + \langle {}^2\Pi_{\frac{3}{2}}|H|{}^2\Pi_{\frac{1}{2}}\rangle F_{\frac{1}{2}}(R) = -\langle {}^2\Pi_{\frac{3}{2}}|H|{}^2\Sigma_{\frac{1}{2}}{}^+\rangle G^+(R), \tag{6}$$

$$\langle {}^2\Sigma_{\frac{1}{2}}{}^+|H-E|{}^2\Sigma_{\frac{1}{2}}{}^+\rangle G^+(R) = -\langle {}^2\Sigma_{\frac{1}{2}}{}^+|H|{}^2\Pi_{\frac{1}{2}}\rangle F_{\frac{1}{2}}(R) - \langle {}^2\Sigma_{\frac{1}{2}}{}^+|H|{}^2\Pi_{\frac{3}{2}}\rangle F_{\frac{3}{2}}(R). \tag{7}$$

Since the Hamiltonian H is diagonal in J, M, and P we shall suppress these indices with the understanding that all matrix elements and functions are implicitly dependent on these quantum numbers.

The expansion in Eq. (1) assumes that the electronic portion of the wavefunction is well described by the $^2\Pi$ state, with a small contribution of $^2\Sigma^+$, while the total spin quantum number $S = \frac{1}{2}$ remains a good quantum number. Given this approximation, the configuration space of the polar coordinates θ, Φ of the internuclear axis, which describes the rotational state of the molecule, is completely spanned by the set of electronic–rotational wavefunctions defined in Eqs. (2) and (3). However, the functional dependence of the total wavefunction with respect to the internuclear coordinate R, which defines the vibrational motion of the molecule, is as yet undetermined and must be obtained from the solution of the coupled equations (5)–(7). These equations only have well-behaved solutions at particular energy eigenvalues $E = E_\alpha$. Of course as $E_\alpha \rightarrow D_e$, where D_e is the dissociation energy of OH(X), the expansion (1) becomes less valid[1] due to the proximity of the excited states such as $^4\Pi$ and $^{2,4}\Sigma^-$. However, for $E_\alpha < D_e/2$ the $^2\Pi$ state is well isolated and (1) should be an excellent approximation. In fact, for the purposes of calculating the vibrational intensities in the X state, we shall neglect the effect of Λ-doubling and assume the $^2\Sigma^+$ radial function G^+ is negligibly small. Perturbative estimates of the error caused by this approximation are made in Appendix A, and except for determination of extremely accurate term values, which is not our intention, the right-hand side of Eqs. (5) and (6) may be set equal to zero and we need only consider the two coupled equations for the radial functions $F_{\frac{1}{2}}$ and $F_{\frac{3}{2}}$. This approximation will become increasingly poor for large J values, and for high vibrational levels.

The total Hamiltonian for the OH system can be written as,

$$H = T_R + H_{AB} + B(R)\mathbf{N}^2 + V_{L\cdot S} \tag{8}$$

where T_R is the nuclear kinetic energy operator,

$$T_R = (-\hbar^2/2\mu R)(\partial^2 R/\partial R^2) \tag{9}$$

[2] The parity of the states due to inversion of the space-fixed coordinates is $I|J,M,P\rangle = P|J,M,P\rangle$. This follows from the phase convention $I\Omega_\Omega{}^{J,M} = e^{-i\pi J}\Omega_\Omega{}^{J,M}$, and the assumption that the electronic functions are constructed such that

$$I|{}^2\Pi;\Lambda,\Sigma\rangle = e^{i\pi/2}|{}^2\Pi;-\Lambda,-\Sigma\rangle \quad \text{and} \quad I|{}^2\Sigma^\pm;0,\Sigma\rangle = \pm e^{i\pi/2}|{}^2\Sigma^\pm;0,-\Sigma\rangle.$$

where μ is the reduced mass $m_H m_0/(m_H + m_0)$, and $\mathbf{N}$ [3] is the nuclear angular momentum operator which when added to the electron orbital angular momentum $\mathbf{L}$ and the electron spin $\mathbf{S}$ yields the total angular momentum $\mathbf{J}$

$$\mathbf{J} = \mathbf{N} + \mathbf{L} + \mathbf{S}. \tag{10}$$

The function $B(R)$ is

$$B(R) = \hbar^2/(2\mu R^2), \tag{11}$$

$V_{L\cdot S}$ is the spin–orbit operator

$$V_{L\cdot S} = A(\mathbf{r}, R)\mathbf{L}\cdot\mathbf{S} \tag{12}$$

and finally H_{AB} is the electronic Hamiltonian for the molecule which generates the electronic wavefunctions and the R-dependent interaction potentials $W(R)$ of the $^2\Pi$ and $^2\Sigma^+$ states,

$$\begin{aligned} H_{AB}|^2\Pi;\Lambda,\Sigma\rangle &= W_\Pi(R)|^2\Pi;\Lambda,\Sigma\rangle, \\ H_{AB}|^2\Sigma^+;0,\Sigma\rangle &= W_{\Sigma^+}(R)|^2\Sigma^+;0,\Sigma\rangle. \end{aligned} \tag{13}$$

We define the R-dependent spin–orbit splitting parameter for the $^2\Pi$ state as follows,

$$\begin{aligned} A(R)\Lambda\cdot\Sigma &= \langle^2\Pi;\Lambda,\Sigma|A(\mathbf{r}, R)\mathbf{L}\cdot\mathbf{S}|^2\Pi;\Lambda,\Sigma\rangle \\ &= \langle^2\Pi;\Lambda,\Sigma|A(\mathbf{r}, R)|^2\Pi;\Lambda,\Sigma\rangle\Lambda\cdot\Sigma. \end{aligned} \tag{14}$$

For OH at R_e $A(R_e) = -139.6$ cm^{-1} (inverted doublet state). The expectation value of $A(\mathbf{r}, R)$ may vary as the nuclear distance is changed; this is likely for OH with its changing degree of charge transfer. Also the splitting will be effected by the proximity of the $^4\Pi$ and $^{2,4}\Sigma^-$ states which asymptotically become degenerate with the $^2\Pi$ state. See for example the analysis of the HF^+ system where the role of this latter phenomenon was considered in the calculation of $H^+ + F(^2P)$ scattering (*19*). Hopefully both these effects can be ignored in the range of 0.8–2.5 Å and in the present analysis we shall assume that $A(R) \approx A(R_e)$. Since $\Lambda = 0$ for the $^2\Sigma^+$ state the expectation value for the spin-orbit operator vanishes. However the spin–orbit interaction does couple the $^2\Pi$ and $^2\Sigma^+$ states, i.e.,

$$A_{\Pi\Sigma}(R) = \langle^2\Pi;1,\Sigma|A(\mathbf{r}, R)L_+|^2\Sigma^+;0,\Sigma\rangle. \tag{15}$$

Estimates of this matrix element have been made by Julienne and Krauss (*20*) and Hinkley *et al.* (*21*) which predict a value at R_e of about -158 cm^{-1}. Again we will ignore any R-dependence in this quantity.

Matrix elements over the kinetic energy operator T_R are diagonal between the six states defined by Eqs. (2) and (3). However, due to the implicit R-dependence of the electronic wavefunctions T_R and these functions do not commute. We shall assume that the expectation value of these radial Born–Oppenheimer breakdown terms are incorporated into an "effective" Π and Σ^+ potential, i.e.,

$$\begin{aligned} \langle^2\Pi_\Omega|T_R|^2\Pi_\Omega\rangle &= T_R + W_\Pi^{\text{eff}}(R) - W_\Pi(R), \\ \langle^2\Sigma_{\frac{1}{2}}^+|T_R|^2\Sigma_{\frac{1}{2}}^+\rangle &= T_R + W_{\Sigma^+}^{\text{eff}}(R) - W_{\Sigma^+}(R). \end{aligned} \tag{16}$$

[3] The nuclear angular moment is often designated as $\mathbf{R}$, however we have used Herzberg's notation (*24*) to avoid confusion with the internuclear coordinate.

Table I. Energy Matrix Elements for Given J,M and Parity P

	$^2\Pi_{3/2}$	$^2\Pi_{1/2}$	$^2\Sigma^+_{1/2}$
$^2\Pi_{3/2}$	$B\,(J-1/2)(J+3/2) + (A/2 - B) + T_R + W_\Pi^{eff}(R)$	$-B\sqrt{(J-1/2)(J+3/2)}$	$-B\,\bar{L}\sqrt{(J-1/2)(J+3/2)}$
$^2\Pi_{1/2}$		$B(J-1/2)(J+3/2) - (A/2 - B) + T_R + W_\Pi^{eff}(R)$	$B\,\bar{L}\left[1 - Pe^{i\pi(J-1/2)}(J+1/2)\right] + 1/2\,A_{\Pi\Sigma}$
$^2\Sigma^+_{1/2}$			$B\left[(J-1/2)(J+3/2) + 1 - Pe^{i\pi(J-1/2)}(J+1/2)\right] + T_R + W_\Sigma^{eff}(R)$

Estimates of such terms have been made by Kolos and Wolniewicz (*22*) for H_2 which indicate these corrections to the Born–Oppenheimer potentials can be of the order of 10^2 cm^{-1}. However the RKR potentials that we shall employ in our calculations are in fact approximations to W^{eff}, rather than W, and even if theoretical W potentials were used, the influence of such terms would be negligible unless the R-dependence of the matrix element influenced the shape of the potential over the required range of R.

Finally we must consider the matrix elements of the nuclear angular momentum,

$$\mathbf{N}^2 = (\mathbf{J}^2 - J_Z^2) + (\mathbf{S}^2 - S_Z^2) + (\mathbf{L}^2 - L_Z^2) \tag{17A}$$

$$- (S_-J_+ + S_+J_-) \tag{17B}$$

$$+ (L_+S_- + L_-S_+ - L_+J_- - L_-J_+) \tag{17C}$$

The terms in (17A) only contribute to diagonal matrix elements; and again we shall incorporate the expectational value of the angular Born–Oppenheimer breakdown term $(\mathbf{L}^2 - L_Z^2)$, which is only dependent on the electronic state, into our definition of an effective potential W^{eff}. Its contribution will be of the order of 20 cm^{-1} for $^2\Pi$ and 40 cm^{-1} for $^2\Sigma^+$.

The second set of terms (17B) couple the $\Omega = \frac{1}{2}$ and $\Omega = \frac{3}{2}$ states of the $^2\Pi$ configuration and give rise to the spin-uncoupling or intermediate coupling,[2]

$$\langle {}^2\Pi_{\frac{1}{2}} | \mathbf{N}^2 | {}^2\Pi_{\frac{3}{2}} \rangle = -\left[(J - \tfrac{1}{2}) \cdot (J + \tfrac{3}{2})\right]^{\frac{1}{2}}. \tag{18}$$

The third set of terms in (17C) couple the Π and Σ^+ state and give rise to Λ-doubling since the matrix elements do depend on the parity P and cause a splitting of the doubly degenerate $P = \pm 1$ states. These terms are proportional to the following electronic matrix element,

$$\bar{L} = \langle {}^2\Pi; 1, \Sigma | L_+ | {}^2\Sigma^+; 0, \Sigma \rangle. \tag{19}$$

This has been calculated (*20*, *21*) to be equal to 1.356 which is close to the value 1.414 expected for a pure $2p_\pi \rightarrow 2p_\sigma$ transition. Table I summarizes the matrix elements that enter Eqs. (5)–(7).

III. APPROXIMATE SOLUTION OF COUPLED EQUATIONS

Numerical techniques are available (*23*) for solving Eqs. (5)–(7) exactly. However it yields more insight into the limitations, and the successes, of the conventional approach to molecular analysis to use a basis set expansion of the following form. Let $|v_0\rangle$ be the complete set of vibrational wavefunctions for the following potential,

$$[T_R + BJ_0(J_0 + 1) + W_{\Pi}^{\text{eff}}(R)]|v_0\rangle = E_{v_0}{}^0|v_0\rangle. \tag{20}$$

The $J_0 = 0$ basis set is normally used to factorize the total wavefunction into a product of vibrational and electronic–rotational functions. Of course $|v_0\rangle$ forms a complete set which spans the space of the nuclear coordinate R, and we can expand the radial functions $F_{\frac{1}{2}}$ and $F_{\frac{3}{2}}$ in this basis,

$$F_\Omega(R) = \sum_{v_0} \mathfrak{A}_{v_0}{}^\Omega|v_0\rangle. \tag{21}$$

A similar expansion in an appropriate $^2\Sigma^+$ basis set can be made for the function $G^+(R)$, as is discussed in Appendix A, but we shall ignore the coupling of the $|^2\Sigma_{\frac{1}{2}}{}^+\rangle$ channel and assume $G^+ = 0$.

Let us represent the matrix elements of the operator 0 by the matrix $\mathbf{0}$, i.e.,

$$\langle v_0|0|v_0'\rangle = 0_{v_0,v_0'} = \mathbf{0}.$$

Substituting Eq. (21) into the coupled equations, and operating from the left with $\langle v_0|$ we obtain the following secular equation,

$$\begin{aligned} [\mathbf{E}^0 - E\cdot\mathbf{1} + \mathbf{S} + \mathbf{D}]\underline{\mathfrak{A}}^{\frac{1}{2}} - \mathbf{C}\underline{\mathfrak{A}}^{\frac{3}{2}} &= 0, \\ [\mathbf{E}^0 - E\cdot\mathbf{1} + \mathbf{S} - \mathbf{D}]\underline{\mathfrak{A}}^{\frac{3}{2}} - \mathbf{C}\underline{\mathfrak{A}}^{\frac{1}{2}} &= 0. \end{aligned} \tag{22}$$

$\mathbf{E}^0 = \delta_{v_0,v_0'}E_{v_0}{}^0$ is the diagonal matrix of vibrational eigenvalues from Eq. (20), $\mathbf{1} = \delta_{v_0,v_0'}$ is the unit matrix, and defining $X^2 = (J - \frac{1}{2})(J + \frac{3}{2})$

$$\begin{aligned} \mathbf{S} &= [X^2 - J_0(J_0 + 1)]\cdot\mathbf{B}, \\ \mathbf{D} &= \mathbf{B} - \tfrac{1}{2}\mathbf{A}, \\ \mathbf{C} &= +X\cdot\mathbf{B}. \end{aligned} \tag{23}$$

The matrices $\underline{\mathfrak{A}}^\Omega = \{\mathfrak{A}_{v_0,\alpha}{}^\Omega\}$ form a set of column vectors for each index α which designates an eigenvalue, $E = E_\alpha(J, M, P)$, that satisfies Eq. (22). These solutions are exact if summed over the infinite set of vibrational states v_0, including the vibrational continuum states. Of course we must truncate the expansion in order to obtain a finite secular equation. In our calculations we have employed the set $v_0 = 0$ to 15 in our analysis and have excluded the continuum states. This truncation is tested against exact numerical solutions in Appendix B, and is found to give excellent solutions for vibrational levels as high as 9, and rotational quantum numbers as large as $J = 16.5$. Note that for each vibrational state included in our expansion two eigenvalues are obtained from (22), or a total of 32 eigenvalues and wavefunctions are determined. For a given J, M, P these eigenvalues separate into pairs of closely spaced eigenvalues which we label with the index $i = 1, 2$, and

$$\alpha = (i, v) \quad \text{with} \quad i = 1, 2 \quad v = 0, 15 \tag{24}$$

where $E_{2,v}(J, M, P) > E_{1,v}(J, M, P)$ and $E_{i,v+\Delta v}(J, M, P) > E_{i,v}(J, M, P)$. $E_{1,v}(J)$ and $E_{2,v}(J)$ then correspond to the $F_1(J, v)$ and $F_2(J, v)$ term values used to describe a $^2\Pi$ state (*24*). These levels are $2\cdot(2J+1)$-fold degenerate, with $-J < M < +J$, and $P = \pm 1$. The accuracy of the calculations are discussed in Section V, and the results are presented in Section VI.

It is convenient to define a linear combination of vibrational–rotational functions which can either go over to the pure Hund's case (b) or can be set equal to Hill and VanVleck's (*15*) intermediate coupling approximation (HVV). Let these functions be designated as $|i, v_0\rangle$, where

$$\begin{aligned} |1, v_0\rangle &= [\sin\Phi_{v_0}|^2\Pi_{\frac{1}{2}}\rangle + \cos\Phi_{v_0}|^2\Pi_{\frac{3}{2}}\rangle]|v_0\rangle, \\ |2, v_0\rangle &= [\cos\Phi_{v_0}|^2\Pi_{\frac{1}{2}}\rangle - \sin\Phi_{v_0}|^2\Pi_{\frac{3}{2}}\rangle]|v_0\rangle. \end{aligned} \tag{25}$$

When $\Phi_{v_0} = \pi/4$ the electronic–rotational factors in (25) represent pure case (b) coupling. Substituting (25) into the expansion (21) we obtain the following equivalent representation of the total wavefunction (1)

$$\begin{aligned} |J, M, P, \alpha\rangle &= \sum_{\Omega}\sum_{v_0} \mathfrak{A}_{v_0,\alpha}{}^{\Omega}|^2\Pi_{\Omega}\rangle|v_0\rangle \\ &= \sum_{i=1,2}\sum_{v_0} \mathfrak{B}_{v_0,\alpha}{}^{i}|i, v_0\rangle \end{aligned} \tag{26}$$

where

$$\begin{aligned} \mathfrak{A}_{v_0,\alpha}{}^{\frac{1}{2}} &= \sin\Phi_{v_0}\mathfrak{B}_{v_0,\alpha}{}^{1} + \cos\Phi_{v_0}\mathfrak{B}_{v_0,\alpha}{}^{2}, \\ \mathfrak{A}_{v_0,\alpha}{}^{\frac{3}{2}} &= \cos\Phi_{v_0}\mathfrak{B}_{v_0,\alpha}{}^{1} - \sin\Phi_{v_0}\mathfrak{B}_{v_0,\alpha}{}^{2}. \end{aligned} \tag{27}$$

We obtain the following equations in the unknown expansion coefficients

$$\begin{aligned} [\mathbf{E}^0 - E\cdot\mathbf{1} + \underline{\mathcal{S}} - \underline{\mathfrak{D}}]\underline{\mathfrak{B}}^1 - \underline{\mathfrak{C}}\,\underline{\mathfrak{B}}^2 = 0, \\ [\mathbf{E}^0 - E\cdot\mathbf{1} + \underline{\mathcal{S}} + \underline{\mathfrak{D}}]\underline{\mathfrak{B}}^2 - \underline{\mathfrak{C}}\,\underline{\mathfrak{B}}^1 = 0, \end{aligned} \tag{28}$$

where the transformed matrices in (28) are defined as follows,

$$\begin{aligned} \mathcal{S}_{v_0,v_0'} &= (\sin\Phi_{v_0}\sin\Phi_{v_0'} + \cos\Phi_{v_0}\cos\Phi_{v_0'})S_{v_0,v_0'}, \\ \mathfrak{D}_{v_0,v_0'} &= (\sin\Phi_{v_0}\cos\Phi_{v_0'} + \cos\Phi_{v_0}\sin\Phi_{v_0'})C_{v_0,v_0'} \\ &\quad + (\cos\Phi_{v_0}\cos\Phi_{v_0'} - \sin\Phi_{v_0}\sin\Phi_{v_0'})D_{v_0,v_0'}, \\ \mathfrak{C}_{v_0,v_0'} &= -(\sin\Phi_{v_0}\cos\Phi_{v_0'} - \cos\Phi_{v_0}\sin\Phi_{v_0'})S_{v_0,v_0'} \\ &\quad - (\sin\Phi_{v_0}\sin\Phi_{v_0'} - \cos\Phi_{v_0}\cos\Phi_{v_0'})C_{v_0,v_0'} \\ &\quad - (\sin\Phi_{v_0}\cos\Phi_{v_0'} + \cos\Phi_{v_0}\sin\Phi_{v_0'})D_{v_0,v_0'}. \end{aligned} \tag{29}$$

The HVV approximation to the exact wavefunction is obtained by choosing the mixing parameter, Φ_{v_0}, in Eq. (25) such that the diagonal coupling term $\mathfrak{C}_{v_0,v_0}$ in Eq. (28) is zero, i.e.,

$$|i, v\rangle \approx |i, v_0\rangle \quad \text{when} \quad \mathfrak{C}_{v_0,v_0} = 0 \text{ (HVV Approximation)}. \tag{30}$$

This approximation will be carefully analyzed in a subsequent paper (*14*).

IV. DIPOLE TRANSITION PROBABILITIES

The total wavefunction $|J, M, P, \alpha\rangle$ in Eq. (26) is characterized by the quantum numbers J, M, P and the index α which labels the eigenvalues $E = E_\alpha$ obtained from

the secular equation (22), or the equivalent equation (28). The wavefunction is defined by the eigenvectors $\mathfrak{A}_{v,\alpha}{}^{\Omega}$ or $\mathfrak{B}_{v,\alpha}{}^{i}$.

The Einstein transition probability for a radiative transition from state $|J', M', P', \alpha'\rangle$ to state $|J'', M'', P'', \alpha''\rangle$ is

$$A(J'', M'', P'', \alpha'' \leftarrow J', M', P', \alpha') = \frac{8\pi\omega^3}{3hc^3} |\langle J', M', P', \alpha' | \mathbf{m} | J'', M'', P'', \alpha'' \rangle|^2 \quad (31)$$

where $\hbar\omega = E_{\alpha'}(J', P') - E_{\alpha''}(J'', P'')$ and $\mathbf{m}$ is the dipole moment of the molecule (we shall use primes to denote space-fixed vector components and unprimed variables to denote molecule-fixed projections), $\mathbf{m} = e[-\sum_i \mathbf{r}_i + \mathbf{R}_H + 8\mathbf{R}_0]$. The vector $\mathbf{m}$ may be represented by its molecule-fixed projections as follows,

$$|\mathbf{m}|^2 = \sum_{\nu=0,\pm1} |m_\nu'|^2 = \sum_{\nu=0,\pm1} \Big| \sum_{\lambda=0,\pm1} m_\lambda D_{\nu,\lambda}{}^{1*}(\Phi, \theta, 0) \Big|^2$$

where m_λ are the molecule-fixed projections of $\mathbf{m}$, and $D_{\nu,\lambda}{}^1$ is the Wigner rotation matrix. For a $^2\Pi \rightarrow {}^2\Pi$ transition matrix elements over $\lambda = \pm 1$ will vanish, and only $\lambda = 0$ is nonvanishing,

$$m_0 = e[-\textstyle\sum_i z_i + Z_H + 8Z_0]. \quad (32)$$

When m_0 is integrated over the electronic wavefunction $|^2\Pi; \Lambda, \Sigma\rangle$ we obtain the dipole moment for the $^2\Pi$ state, which is a function of the internuclear coordinate $R = Z_H - Z_0$.

$$d(R) = \langle {}^2\Pi; \Lambda, \Sigma | m_0 | {}^2\Pi; \Lambda, \Sigma \rangle. \quad (33)$$

This dipole moment has been evaluated to very high accuracy by Stevens *et al.* (*10*) and is reproduced in Fig. 1. Let

$$R_{v_0, v_0'} = \langle v_0 | d(R) | v_0' \rangle. \quad (34)$$

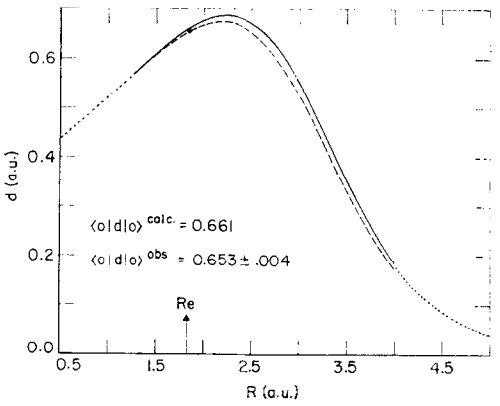

FIG. 1. Theoretical dipole moment function, $d(R)$, for OH($X^2\Pi$) calculated by Stevens, Das, Wahl, Neumann and Krauss (*11*). The solid curve between $1.5 < R < 4.0$ is a spline fit to their best results obtained with a 17-configuration basis set. The dashed curve is a fit to their 14-configuration data. The dotted curves in the regions $1.5 > R > 4.0$ are arbitrary extrapolations used in the present calculations; however the results are insensitive to the form of $d(R)$ in these regions. The derived experimental dipole moment at R_e is shown by the data point which falls between the two theoretical curves. The $v = 0$ expectation value of $d(R)$ is shown.

This matrix defines the vibrational transition probabilities for the basis set $|v_0\rangle$. The resultant expression for the Einstein coefficient is,

$$A(J'', M'', P'', \alpha'' \leftarrow J', M', P', \alpha') = \frac{8\pi\omega^3}{3hc^3}\left[\sum_{\nu}\left(\frac{2J'+1}{2J''+1}\right)C(J', 1, J''; M', \nu, M'')^2\right]\mathcal{P}^2, \quad (35)$$

where

$$\mathcal{P} = \tfrac{1}{2}[1 - P'P''] \sum_{\Omega', \Omega'', v_0', v_0''} \mathfrak{A}_{v_0', \alpha'}{}^{\Omega'*}\mathfrak{A}_{v_0'', \alpha''}{}^{\Omega''}C(J', 1, J''; \Omega', \Omega'' - \Omega', \Omega'') \times\{R_{v_0', v_0''}\delta_{\Omega', \Omega''}\}. \quad (36)$$

We define a total transition probability, averaged over initial M' angular momentum projections and parities P' and summed over final M'' projections, and parities P''.

$$\bar{A}(J'', \alpha'' \leftarrow J'\alpha') = \sum_{M'', M', P'', P'} \frac{A(J'', M'', P'', \alpha'' \leftarrow J', M', P', \alpha')}{2\cdot(2J'+1)}.$$

Using the fact that the Clebsch–Gordan coefficients $C(J', 1, J''; M', \nu, M'')^2$ summed over M', M'' and ν yield $(2J''+1)$, we obtain the following result for $\bar{A}$

$$\bar{A}(J'', \alpha'' \leftarrow J', \alpha') = (8\pi\omega^3/3hc^3)\mathcal{P}^2. \quad (37)$$

Recall that the coefficients $\mathfrak{A}_{v_0', \alpha'}{}^{\Omega'} = \mathfrak{A}_{v_0', \alpha'}{}^{\Omega'}(J', P')$ are implicit functions of the quantum numbers J' and P' (in the absence of Λ-doubling they depend only on J' and are independent of the parity P'). The usual selection rules are obtained from (37), i.e., $P'' \neq P'$ and $J'' = J', J' \pm 1$.

The various special cases for Hund's cases (a) and (b) or Hill and VanVleck's intermediate coupling (*15*) are easily derived from (37) by using appropriate approximations for the coefficients $\mathfrak{A}_{v,\alpha}{}^{\Omega}$.

If we assume a Boltzmann distribution of initial doublet states, $i' = 1, 2$ in Eq. (24), and a Boltzmann distribution of rotational states J', both at a temperature T_{rot}, then we may define a thermally averaged radiative transition probability for the vibrational band $v'' \leftarrow v'$ which is averaged over initial i', J' states and summed over all final i'', J''[3] states,

$$A_{v''\leftarrow v'}(T_{\text{rot}}) = \sum_{i', J', i'', J''} \bar{A}(J'', i'', v'' \leftarrow J', i', v')\frac{2(2J'+1)}{Q_{v'}(T_{\text{rot}})}\exp\left\{\frac{-E_{i',v'}(J')}{kT_{\text{rot}}}\right\}. \quad (38)$$

$Q_{v'}(T_{\text{rot}})$ is the electronic–rotational partition function for the v' level,

$$Q_{v'}(T_{\text{rot}}) = \sum_{J', i'} 2(2J'+1)\exp\left\{\frac{-E_{i',v'}(J')}{kT_{\text{rot}}}\right\}. \quad (39)$$

If $N_{v'}$ is the total concentration of OH molecules in the v' state, then $A_{v''\leftarrow v'}(T_{\text{rot}})N_{v'}$ is the total rate at which radiative transitions occur between v' and v''.

The integrated absorption coefficient $\bar{S}(J'', i'', v'' \rightarrow J', i', v')$ has the units of Amagat^{-1} cm^{-2} and is related to $\bar{A}(J'', i'', v'' \leftarrow J', i', v')$ as follows

$$\bar{S}(J'', i'', v'' \rightarrow J', i', v') = 3.567 \times 10^7 (2J' + 1)\bar{A}(J'', i'', v'' \leftarrow J', i', v')/(2J'' + 1)\bar{\nu}^2 \quad (40)$$

where $\bar{\nu}hc = E_{i',v'}(J') - E_{i'',v''}(J'')$. A thermally averaged integrated absorption coefficient, $S_{v'' \rightarrow v'}(T_{\text{rot}})$ may be defined, in analogy to $A_{v'' \leftarrow v'}(T_{\text{rot}})$ in Eq. (38), but with a Boltzmann average over the i'', J'' states and a summation over the final i', J' states.

V. ACCURACY OF CALCULATIONS

A. Accuracy of Eigenvalues and Wavefunctions

Given accurate values for the matrix elements $A_{v_0,v_0'}$, $B_{v_0,v_0'}$ and $E_{v_0}{}^0$ which define the secular equation (22) we may determine the total eigenvalue $E_\alpha(J, M, P)$ and the total wavefunction $|J, M, P, \alpha\rangle$. The accuracy of the expansion (21) for vibrational quantum numbers $\leqslant 9$, and angular momentum $J \leqslant 16.5$ is tested in Appendix B, and indicates that eigenvalues should be exact to within ± 0.1 cm^{-1}, and transition matrix elements should be accurate to at least 1%. This is further confirmed by the agreement obtained in our final results using three different basis sets generated by Eq. (20), with $J_0 = 0$, 5, 10. The resultant eigenvalues $E_\alpha(J)$ for quantum states $\alpha \equiv (i, v)$ all agree to within .01 cm^{-1} for $v < 9$, and $J < 16.5$, with the restriction $J_0 < J$. [As indicated in Appendix B, less accurate results are obtained if $J_0 > J$ due to the increased importance of the neglected vibrational continuum states in the expansion (21).] More importantly, using the three different basis sets, the calculated transition probabilities $\bar{A}(J'', i'', v'' \leftarrow J', i', v')$ obtained from Eq. (37) agree to within $\sim 0.1\%$ for the intra-multiplet transitions, $i'' = i'$, and agree to within $\sim 1\%$ for the weaker, and more sensitive satellite transitions, $i'' \neq i'$.

Two quantities are needed as input to the calculation of the matrices **A**, **B**, and $\mathbf{E}^0$; (i) the molecular potential $W_\Pi{}^{\text{eff}}(R)$ which defines the vibrational basis set, $|v_0\rangle$, and zero-order eigenvalues, $E_{v_0}{}^0$, of Eq. (20); and (ii) the spin–orbit interaction $A(R)$.

(i) For $W_\Pi{}^{\text{eff}}(R)$ we have employed the RKR potential calculated by Albritton (*13*) from a Dunham analysis of the $^2\Pi$ state. This potential agrees to within 0.2 eV at R_e with an accurate MCSCF calculation (*10*) of $W_\Pi(R)$, and over the important range of $R = 0.6$–2.5 Å the two curves are parallel to within 0.10 eV. As inferred in Section II, $W_\Pi{}^{\text{eff}}$ is actually the adiabatic Born potential since it contains the diagonal expectatino value of the Born–Oppenheimer break-down terms arising from the kinetic energy operator T_R; however such terms are negligible compared to the inaccuracies of the theoretical potential and they should have an insignificant effect on the relative shapes of W_Π(calc) and $W_\Pi{}^{\text{eff}}$(RKR). Obviously the RKR analysis offers a more accurate input for $W_\Pi{}^{\text{eff}}(R)$. Primarily the excellent agreement with the theoretical potential is emphasized because it lends additional confidence in the accuracy of the dipole moment function $d(R)$ that we have used and which is derived from the same theoretical calculations.

(ii) The spin–orbit interaction $A(R)$ is obtained from Moore and Richard's re-analysis (*25*) of the $X^2\Pi$ data; the analysis is based on the HVV approximation which includes the assumption that $A(R) = A(R_e)$ is a constant. The equilibrium value

Table II. Comparison of present calculations to R.K.R. properties.

v	E_v^{RKR}	$E_v^{Calc.}$	$B_{v,v}^{RKR}$	$B_{v,v}^{Calc.}$
0	1851.33	1850.73	18.520	18.520
1	5421.02	5420.17	17.802	17.803
2	8824.80	8823.51	17.103	17.102
3	12065.08	12063.77	16.416	16.414
4	15142.98	15141.81	15.733	15.729
5	18058.32	18057.48	15.047	15.041
6	20809.61	20809.21	14.351	14.345
7	23394.1	23393.78	13.64	13.63
8	25807.6	25806.93	12.90	12.90
9	28044.7	28042.89	12.13	12.14
10		30093.77		11.34
11		31946.85		10.47

should be adequately determined from the $J = \frac{3}{2}$ and $v = 0$ term values and is given as -139.37 cm^{-1}. Any error introduced into our calculations by assuming A is independent of R is negligible if the off-diagonal elements of the matrix **A** are small compared to **B**. This assumption should be particularly valid for a hydride such as OH. Walker and Richards (*26*) have calculated the OH spin–orbit constant and find it differs by only 5 cm^{-1} from the atomic value, and therefore we expect that A will be an insignificantly varying function of R, with negligible off-diagonal matrix elements.

Table III. $B_{v,v'}$(cm^{-1}) matrix elements for J_o=0

v \ v'	0	1	2	3	4	5	6	7
0	0.18520+02	0.25623+01	0.65702+00	0.21334+00	0.80309-01	0.34086-01	0.15706-01	0.77978-02
1	0.25625+01	0.17802+02	0.34568+01	0.10777+01	0.40132+00	0.16841+00	0.77399-01	0.38365-01
2	0.65705+00	0.34566+01	0.17102+02	0.40366+01	0.14437+01	0.59707+00	0.27330+00	0.13547+00
3	0.21333+00	0.10777+01	0.40365+01	0.16413+02	0.44406+01	0.17649+01	0.79622+00	0.39243+00
4	0.80347-01	0.40126+00	0.14436+01	0.44404+01	0.15729+02	0.47207+01	0.20473+01	0.99408+00
5	0.34077-01	0.16841+00	0.59708+00	0.17649+01	0.47206+01	0.15040+02	0.49059+01	0.22904+01
6	0.15710-01	0.77430-01	0.27330+00	0.79622+00	0.20473+01	0.49059+01	0.14344+02	0.50128+01
7	0.77781-02	0.38397-01	0.13549+00	0.39244+00	0.99411+00	0.22903+01	0.50128+01	0.13633+02
8	0.42292-02	0.20375-01	0.71756-01	0.20753+00	0.52249+00	0.11858+01	0.24964+01	0.50501+01
9	0.22946-02	0.11428-01	0.40407-01	0.11676+00	0.29293+00	0.65996+00	0.13681+01	0.26628+01
10	0.13718-02	0.68068-02	0.23977-01	0.69282-01	0.17358+00	0.38984+00	0.80197+00	0.15369+01
11	0.85579-03	0.42713-02	0.14942-01	0.43169-01	0.10808+00	0.24240+00	0.49658+00	0.94410+00
12	0.46240-03	0.27685-02	0.98325-02	0.28283-01	0.70584-01	0.15804+01	0.32299+00	0.61138+00
13	0.32245-03	0.19028-02	0.66680-02	0.19178-01	0.47837-01	0.10709+00	0.21852+00	0.41251+00
14	0.17098-03	0.13103-02	0.46838-02	0.13404-01	0.33310-01	0.74477-01	0.15180+00	0.28611+00
15	0.13359-03	0.90134-03	0.32001-02	0.91551-02	0.22767-01	0.50875-01	0.10364+00	0.19513+00

v \ v'	8	9	10	11	12	13	14	15
0	0.42862-02	0.22939-02	0.13506-02	0.86160-03	0.46415-03	0.34662-03	0.17862-03	0.13815-03
1	0.20372-01	0.11430-01	0.67985-02	0.42739-02	0.27762-02	0.19098-02	0.13118-02	0.90689-03
2	0.71733-01	0.40400-01	0.23987-01	0.14942-01	0.98248-02	0.66582-02	0.46733-02	0.31955-02
3	0.20748+00	0.11675+00	0.69305-01	0.43168-01	0.28282-01	0.19156-01	0.13415-01	0.91521-02
4	0.52248+00	0.29295+00	0.17358+00	0.10809+00	0.70582-01	0.47837-01	0.33310-01	0.22757-01
5	0.11858+01	0.65998+00	0.38980+00	0.24239+00	0.15804+00	0.10709+00	0.74460-01	0.50870-01
6	0.24965+01	0.13681+01	0.80194+00	0.49659+00	0.32299+00	0.21855+00	0.15180+00	0.10365+00
7	0.50501+01	0.26628+01	0.15369+01	0.94411+00	0.61140+00	0.41253+00	0.28612+00	0.19514+00
8	0.12901+02	0.50208+01	0.27880+01	0.16865+01	0.10836+01	0.72768+00	0.50333+00	0.34268+00
9	0.50209+01	0.12140+02	0.49264+01	0.28666+01	0.18138+01	0.12083+01	0.83203+00	0.56494+00
10	0.27880+01	0.49265+01	0.11336+02	0.47617+01	0.28985+01	0.19015+01	0.12991+01	0.87828+00
11	0.16866+01	0.28666+01	0.47616+01	0.10469+02	0.45259+01	0.28543+01	0.19219+01	0.12902+01
12	0.10836+01	0.18138+01	0.28985+01	0.45259+01	0.95507+01	0.42011+01	0.27157+01	0.17972+01
13	0.72773+00	0.12083+01	0.19015+01	0.28542+01	0.42012+01	0.85275+01	0.37517+01	0.23842+01
14	0.50339+00	0.83202+00	0.12991+01	0.19219+01	0.27157+01	0.37517+01	0.73217+01	0.30544+01
15	0.34269+00	0.56490+00	0.87827+00	0.12902+01	0.17972+01	0.23841+01	0.30544+01	0.57108+01

The eigenvalues $E_{v_0}{}^0(J_0)$ and the eigenfunctions $|v_0\rangle$ generated by Eq. (20), for prescribed values of J_0, and using Albritton's (*13*) RKR potential, are calculated numerically using a program (*27*) based on the Gordon (*23*) algorithm. Basis sets were generated for $J_0 = 0$, 5, and 10 and the matrix elements $B_{v_0,v_0'}(J_0)$ of Eq. (11) were evaluated. A comparison is made in Table II between the results of our numerical solutions of (20) for $J_0 = 0$ and the quantities $E_{v_0}{}^{\mathrm{RKR}}$ and $B_{v_0,v_0}{}^{\mathrm{RKR}}$ obtained from the RKR analysis. The eigenvalues agree to within our prescribed convergence criterion of 1 cm^{-1} and our subsequent calculations of vibrational–rotational term values are uncertain by this amount for small J, and by larger amounts as J, and the neglected Λ-doubling contributions, increases. However we do expect that the vibrational wavefunctions are of sufficient accuracy that matrix elements such as $B_{v_0,v_0'}$ and $R_{v_0,v_0'}$ are insensitive to further refinements in our numerical solutions. The accuracy of the final wavefunctions is directly dependent on the accuracy of $B_{v_0,v_0'}$. Table II indicates the excellent agreement between our calculated diagonal matrix elements and the RKR rotational constants $B_{v_0,v_0}{}^{\mathrm{RKR}}$. The $B_{v_0,v_0'}$ matrix for $J_0 = 0$ is presented in Table III. An indication of the numerical accuracy of our numerical integration procedures is obtained by comparing the elements $B_{v_0,v_0'}$ and B_{v_0',v_0} which should be identical for the symmetric matrix **B**. These elements are evaluated with different integration steps and grid points and generally agree to better than 5×10^{-5} cm^{-1}. Calculations were performed with more accurate wavefunctions and they substantiate this conclusion that the **B** matrix elements are accurately evaluated to within .00005 cm^{-1}. This would introduce a negligible inaccuracy in the final results.

B. Accuracy of Dipole Transition Probabilities

The accuracy of the emission intensities is dependent on the accuracy of the dipole moment function $d(R)$ in Eq. (33) which is then used to evaluate the matrix **R** in (34), and ultimately the Einstein coefficients as expressed in Eq. (37). The dipole moment function has been calculated by Stevens *et al.* (*10*). Their most accurate result, based on a 17-configuration MCSCF calculation, is shown by the solid curve in Fig. 1. The curve represents a spline fit to the 14 values of $d(R)$ that were evaluated between 1.25 and 4.0 a.u. Various arbitrary extrapolations were made of the function outside this range of R, and for $v \leqslant 10$ the calculated $R_{v_0,v_0'}$ matrix elements were found to be invariant to within .00001 a.u. The more significant uncertainty is in the accuracy of the calculated dipole moment function. For example, the dashed curve in Fig. 1 represents a spline fit to the slightly less accurate 14-configuration results presented by Stevens *et al.* A comparison is made in Table IV between the R matrix elements evaluated with these two functions, using the $J_0 = 0$ basis set. These are plotted in Fig. 2 for $\Delta v = 1$ and 2. The most pronounced changes occur in the $R_{v,v+1}$ matrix elements which relate most directly to the fundamental intensities in OH. As a function of v the element changes sign between $v = 4$ and 5, which is indicative of significant differencing effects occurring in the numerical integration. On the other hand the $\Delta v = 2$, 3, 4 matrix elements are relatively insensitive to the improvement in the dipole moment function. However the conclusion of Stevens *et al.* (*10*) is that it would be difficult to imagine any improvements in the 17-configuration wavefunction that would significantly influence the resultant dipole moment.

Table IV. Variation of $R_{v,v'}$ matrix with dipole moment function

v	$R_{v,v}$	$R_{v,v+1}$	$R_{v,v+2}$	$R_{v,v+3}$	$R_{v,v+4}$	$R_{v,v+5}$	$R_{v,v+6}$
0	0.6609+00[a]	-0.1410-01	-0.4471-02	-0.6463-03	-0.1374-03	-0.7303-04	-0.6035-04
0	0.6527+00[b]	-0.1207-01	-0.4581-02	-0.8467-03	-0.2709-03	-0.9928-04	-0.9016-05
1	0.6635+00	-0.1671-01	-0.8105-02	-0.1507-02	-0.3037-03	-0.8554-04	-0.5105-04
1	0.6538+00	-0.1383-01	-0.8218-02	-0.1681-02	-0.4097-03	-0.1206-03	-0.8013-05
2	0.6639+00	-0.1592-01	-0.1178-01	-0.2562-02	-0.5983-03	-0.1674-03	-0.5787-04
2	0.6526+00	-0.1209-01	-0.1182-01	-0.2731-02	-0.6479-03	-0.1957-03	-0.4774-04
3	0.6617+00	-0.1224-01	-0.1559-01	-0.3902-02	-0.9829-03	-0.3302-03	-0.1181-03
3	0.6489+00	-0.7478-02	-0.1541-01	-0.4160-02	-0.1017-02	-0.3327-03	-0.1248-03
4	0.6565+00	-0.5781-02	-0.1935-01	-0.5673-02	-0.1508-02	-0.5158-03	-0.2269-03
4	0.6420+00	-0.2911-03	-0.1874-01	-0.6058-02	-0.1599-02	-0.4794-03	-0.2129-03
5	0.6476+00	0.3528-02	-0.2276-01	-0.7973-02	-0.2302-02	-0.7801-03	-0.3514-03
5	0.6317+00	0.9365-02	-0.2147-01	-0.8394-02	-0.2564-02	-0.7576-03	-0.2752-03
6	0.6346+00	0.1568-01	-0.2535-01	-0.1080-01	-0.3527-02	-0.1218-02	-0.5390-03
6	0.6177+00	0.2140-01	-0.2326-01	-0.1098-01	-0.3976-02	-0.1373-02	-0.4821-03
7	0.6169+00	0.3060-01	-0.2656-01	-0.1403-01	-0.5367-02	-0.2031-02	-0.8706-03
7	0.5993+00	0.3588-01	-0.2382-01	-0.1374-01	-0.5766-02	-0.2392-02	-0.1021-02
8	0.5939+00	0.4801-01	-0.2561-01	-0.1734-01	-0.7332-02	-0.3440-02	-0.1590-02
8	0.5759+00	0.5267-01	-0.2234-01	-0.1654-01	-0.8063-02	-0.3774-02	-0.1881-02

[a] Elements obtained with 17-configuration dipole moment function

[b] Elements obtained with 14-configuration dipole moment function

The full 17-configuration R matrix for $J_0 = 0$ is given in Table V. The degree of symmetry (to within about .000001 a.u.) is a measure of the numerical accuracy of the integration. However because of the sensitivity of this matrix to small changes in $d(R)$ as shown in Table IV and Fig. 2, we must give less credibility to elements with magnitudes less than about 0.1×10^{-3} a.u. Generally the calculated transition probabilities

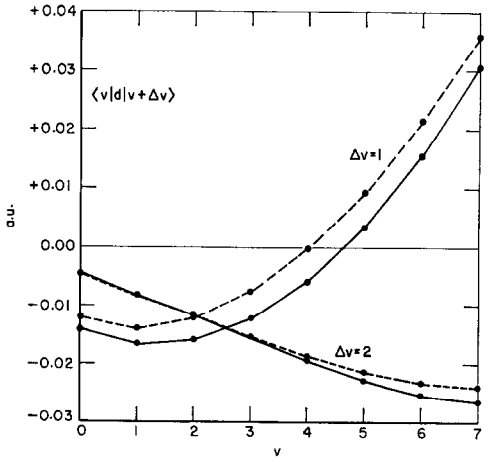

FIG. 2. Vibrational dipole matrix elements, $R_{v,\Delta v+v} = \langle v \,|\, d(R) \,|\, v + \Delta v \rangle$, for the fundamental, $\Delta v = 1$, and first overtone, $\Delta v = 2$, transitions. The solid curve is calculated using the theoretical, 17-configuration dipole moment function in Fig. 1, while the dashed curve is obtained with the slightly less accurate 14-configuration function. The fundamental curve passes through zero and is very sensitive to the seemingly small variation in $d(R)$. The $3 \leftarrow 4$, $4 \leftarrow 5$, and $5 \leftarrow 6$ transitions are especially sensitive, and subject to large rotation–vibration coupling effects.

Table V. $R_{v,v'}$ (a.u.) matrix elements for J_o=0.

v \ v'	0	1	2	3	4	5	6	7
0	0.66089+00	-0.14102-01	-0.44709-02	-0.64631-03	-0.13740-03	-0.73028-04	-0.60347-04	-0.31468-04
1	-0.14099-01	0.66354+00	-0.16711-01	-0.81046-02	-0.15074-02	-0.30370-03	-0.85535-04	-0.51045-04
2	-0.44685-02	-0.16715-01	0.66386+00	-0.15920-01	-0.11777-01	-0.25615-02	-0.59831-03	-0.16736-03
3	-0.64697-03	-0.81053-02	-0.15922-01	0.66170+00	-0.12243-01	-0.15590-01	-0.39023-02	-0.98294-03
4	-0.13610-03	-0.15075-02	-0.11779-01	-0.12246-01	0.65648+00	-0.57808-02	-0.19346-01	-0.56733-02
5	-0.72703-04	-0.30414-03	-0.25618-02	-0.15590-01	-0.57792-02	0.64764+00	0.35279-02	-0.22760-01
6	-0.60294-04	-0.84917-04	-0.59751-03	-0.39025-02	-0.19346-01	0.35284-02	0.63464+00	0.15675-01
7	-0.31143-4	-0.49887-04	-0.16716-03	-0.98311-03	-0.56732-02	-0.22759-01	0.15676-01	0.61693+00
8	0.46323-05	-0.40510-04	-0.56731-04	-0.32888-03	-0.15074-02	-0.79733-02	-0.25347-01	0.30596-01
9	0.20709-04	-0.26216-04	-0.33136-04	-0.11807-03	-0.51593-03	-0.23021-02	-0.10797-01	-0.26558-01
10	0.27423-04	-0.55281-05	-0.31760-04	-0.42272-04	-0.22692-03	-0.78033-03	-0.35277-02	-0.14034-01
11	0.24758-04	0.11285-04	-0.26916-04	-0.21344-04	-0.10437-03	-0.35150-03	-0.12191-02	-0.53670-02
12	0.14444-04	0.18133-04	-0.14189-04	-0.16151-04	-0.44122-04	-0.18812-03	-0.53929-03	-0.20310-02
13	0.85601-05	0.20634-04	-0.37813-05	-0.17783-04	-0.20150-04	-0.10221-03	-0.29896-03	-0.87092-03
14	0.10209-05	0.17644-04	0.54146-05	-0.13875-04	-0.10348-04	-0.56029-04	-0.18796-03	-0.45655-03
15	-0.10434-05	0.13514-04	0.83151-05	-0.10827-04	-0.73543-05	-0.30435-04	-0.11676-03	-0.27049-03

v \ v'	8	9	10	11	12	13	14	15
0	0.58441-05	0.20760-04	0.27271-04	0.25564-04	0.14783-04	0.93576-05	0.18076-05	-0.36175-06
1	-0.40293-04	-0.26247-04	-0.55759-05	0.11276-04	0.18402-04	0.21035-04	0.17716-04	0.13747-04
2	-0.57876-04	-0.33250-04	-0.31522-04	-0.26833-04	-0.14316-04	-0.38948-05	0.51579-05	0.80250-05
3	-0.33024-03	-0.11808-03	-0.42025-04	-0.21660-04	-0.16328-04	-0.18226-04	-0.14131-04	-0.11159-04
4	-0.15076-02	-0.51575-03	-0.22679-03	-0.10393-03	-0.44191-04	-0.20139-04	-0.10436-04	-0.76337-05
5	-0.79726-02	-0.23018-02	-0.78011-03	-0.35136-03	-0.18791-03	-0.10206-03	-0.56341-04	-0.30398-04
6	-0.25347-01	-0.10797-01	-0.35270-02	-0.12184-02	-0.53899-03	-0.29834-03	-0.18741-03	-0.11575-03
7	0.30598-01	-0.26558-01	-0.14034-01	-0.53666-02	-0.20310-02	-0.87060-03	-0.45625-03	-0.26992-03
8	0.59391+00	0.48012-01	-0.25605-01	-0.17341-01	-0.79316-02	-0.34401-02	-0.15898-02	-0.80265-03
9	0.48015-01	0.56493+00	0.67618-01	-0.21506-01	-0.20120-01	-0.11103-01	-0.56580-02	-0.29141-02
10	-0.25605-01	0.67619-01	0.52916+00	0.88643-01	-0.13073-01	-0.20949-01	-0.14208-01	-0.83041-02
11	-0.17341-01	-0.21506-01	0.88642-01	0.48565+00	0.10964+00	0.46570-03	-0.17535-01	-0.14737-01
12	-0.79320-02	-0.20120-01	-0.13071-01	0.10964+00	0.43463+00	0.12793+00	0.19836-01	-0.68165-02
13	-0.34397-02	-0.11103-01	-0.20949-01	0.46615-03	0.12793+00	0.37436+00	0.14008+00	0.43414-01
14	-0.15896-02	-0.56579-02	-0.14208-01	-0.17536-01	0.19838-01	0.14009+00	0.30247+00	0.13550+00
15	-0.80290-03	-0.29144-02	-0.83039-02	-0.14738-01	-0.68149-02	0.43415-01	0.13550+00	0.21037+00

should be most accurate for $\Delta v = 1, 2$, and 3 and with decreasing but probably significant accuracy for $\Delta v = 4$ and 5. However, with regard to specific transitions, the safest course would be to use Table IV as a measure of confidence; those elements which exhibit substantial sensitivity to a change in $d(R)$ are least to be trusted. In particular, the fundamental transitions 6–5, 5–4, and 4–3 are very sensitive to changes in $d(R)$. However, there is one important qualification with regard to this criterion. Because of the significant rotation–vibration interaction in OH, the vibrational wavefunctions for differing J states are nonorthogonal and the P and R branch intensities receive significant contributions from several **R** matrix elements. Accordingly the expected accuracy may be increased or decreased depending on the constructive or destructive interference between these elements. This is especially true for the fundamental transitions as is discussed in the following section.

VI. PRESENTATION AND DISCUSSION OF RESULTS

A. Specific Rotational–Vibrational Transition Probabilities

Using the solutions of Eq. (22), and the quantum numbers $\alpha = (i, v)$ defined by Eq. (24), we have calculated the Einstein coefficients $\bar{A}(J'', i'', v'' \leftarrow J', i', v')$ defined by Eq. (37). The intramultiplet transitions, $i'' = i'$, are tabulated in Appendix C, for $v' = 1$, 9 and $v'' = v' - \Delta v$, where $\Delta v = 1$, 2, 3, 4, and 5. The specific rotational band intensities are labelled $P_{i'}(J')$, $Q_{i'}(J')$ and $R_{i'}(J')$ for $J'' = J' + 1$, J' and $J' - 1$ respectively.[4] The intermultiplet transitions, $i'' \neq i'$, which are called the satellite

[4] Primed quantum numbers always designate upper states, and double primed numbers refer to lower states. Since we are primarily interested in emission all $P(J')$, $Q(J')$ and $R(J')$ branches are labelled according to the total angular momentum J' of the *upper* state.

bands and designated by $P_{i'i''}(J')$, etc., are generally much weaker and are not presented in this paper. However, they are discussed in detail in (*14*) since they are very sensitive to small variations in the wavefunctions and serve as a useful measure of rotational–vibrational coupling effects (*16*), and also of deviations from the HVV approximation (*15*).

Two features are quite prominent in this tabulation of intensities. First, the first overtone bands, $\Delta v = 2$, except for $v' = 2$, are *more* intense than the fundamental bands, $\Delta v = 1$. This effect has been observed experimentally by Murphy (*11*). The ratio of specific P branch intensities in the overtone vs the fundamental band have been measured for $v' = 2$ and $v' = 3$. These transitions originate from the same upper state and are therefore independent of concentration effects and temperature. An averaged value of 0.44 ± 0.03 is quoted for the $P_{i'}(J')^{0\leftarrow 2}/P_{i'}(J')^{1\leftarrow 2}$ transition, with $J' = 0.5$–6.5. The theoretical average for these ratios is 0.46 ± 0.06. The averaged experimental value for the $P_{i'}{}^{1\leftarrow 3}/P_{i'}{}^{2\leftarrow 3}$ ratio is given as 1.15 ± 0.05 while the theoretical value ranges from 1.34 to 2.44 with an averaged value of 1.62. Considering the uncertainties in the theoretical dipole moment, and the possible systematic errors and often poor signal to noise ratio in the experimental measurements, the agreement can be judged as satisfactory. The Q-branch ratio $Q^{2\leftarrow 4}/Q^{3\leftarrow 4}$ is measured to be 3.3 ± 0.7, but is not resolved into individual rotational lines, and has a signal to noise ratio of about 1. The theoretical value is 7.8 and is subject to possible error since the $3 \leftarrow 4$ transition is quite sensitive to changes in the theoretical transition moment (see Table IV).

The second prominent feature of the theoretical intensities is the marked influence of vibrational couplings on the relative intensities in the P, Q and R branches of a given band, especially in the fundamental bands. This is discussed in detail in Ref. (*14*). A detailed comparison has been made between the entire experimental spectrum obtained by Murphy (private communication of unpublished data employed in (*14*)) and the theoretically predicted, Boltzmann averaged, spectrum at $T = 450$ K. The comparison within any given band, for $v' = 1, 2, 3$ and $\Delta v = 1, 2$ is extraordinarily good, and gives an overall impression of almost exact agreement between theory and experiment with regard to the multiplet-rotational line strengths. In particular the predictions are in quantitative agreement with Murphy's measurements of the $2 \leftarrow 3$ and $1 \leftarrow 3$ P, Q- and R-branch intensities and substantiate the observation that the R branch intensities are anomalously weak. An interesting effect of the change in sign of the matrix element $R_{v',v'-1}$ as v' increases (see Table IV and Fig. 2) is that at higher v' and P branch intensity becomes anomalously small and the R branch is much more intense. This difference in qualitative behavior is shown in Fig. 3 where we have plotted the predicted $6 \leftarrow 7$ band and the $2 \leftarrow 3$ band emission spectra at 450 K.

B. Line Strengths and the Determination of Rotational Temperatures

Rotational temperatures for OH are often determined from the intensity distribution of the rotational lines. For a Boltzmann distribution of multiplet rotational levels, the photon intensity (photons/sec cm^3) is given by the following expression,

$$I(J'', i', v'' \leftarrow J', i', v') = N_{v'}\bar{A}(J'', i', v'' \leftarrow J', i', v')\frac{2(2J'+1)}{Q_{v'}(T_{\text{rot}})}\exp\left[\frac{-E_{i',v'}(J')}{kT_{\text{rot}}}\right], \quad (41)$$

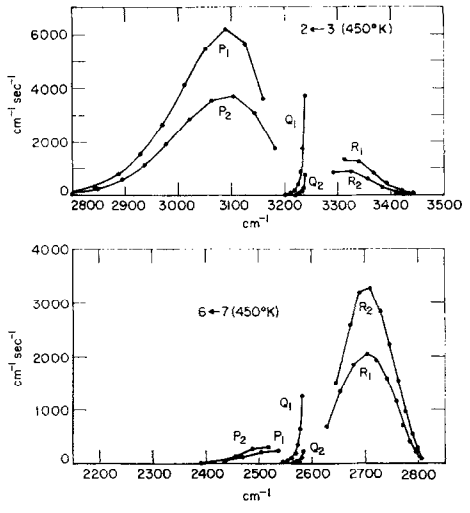

FIG. 3. Demonstration of rotation–vibration coupling effects in the fundamental bands of OH. The calculated rotational line intensities (energy/sec) for a multiplet-rotational temperature of 450 K are plotted for the $2 \leftarrow 3$ and the $6 \leftarrow 7$ vibrational bands. The marked change in relative intensities of the P and R branches within each band is due to the difference in sign of the vibrational transition matrix elements for the two transitions (see Fig. 2).

where $N_{v'}$ is the total concentration of molecules in the v' vibrational level, and $Q_{v'}$ is the partition function defined in Eq. (39). However, the intensities are generally analyzed by approximating the Einstein coefficients in Eq. (37) as follows (*6*),

$$\tilde{A}(J'', i', v'' \leftarrow J', i', v') \approx \left(\frac{8\pi\omega^3}{3hc^3}\right) P_{v',v''} S_{J'',J'}{}^{i'} F_{v'',J''\leftarrow v',J'}. \tag{42}$$

In all cases the so-called Herman–Wallis factor F, which is a perturbative correction factor for the vibrational-rotational coupling effects, is ignored ($F = 1$). In many cases the rotational line strengths $S_{J'',J'}{}^{i'}$ are approximated by the Hönl–London formulae, which only apply to pure Hund's case (a) coupling, or at best the Benedict, Plyler and Humphreys (*28*) tabulation of very *approximate* Hill and VanVleck (*15*) intermediate coupling line strengths are employed.[5] The assumption is then made that

$$\ln\left[\frac{I(J'', i', v'' \leftarrow J', i', v')}{S_{J'',J'}{}^{i'}(2J' + 1)N_{v'}\omega^3}\right] = C(v'' \leftarrow v') - E_{i',v'}(J')/kT_{\text{rot}} \tag{43}$$

and a plot of the *LHS* of Eq. (43) vs the upper state term values $E_{i'v'}(J')$ for a particular vibrational band $v'' \leftarrow v'$ will yield a slope equal to $1/kT_{\text{rot}}$.

It should be obvious from Fig. 3 that this procedure can lead to serious error since the rotational line strengths $S_{J'',J'}{}^{i'}$ employed in Eq. (43) completely misrepresent the true fundamental line strength distributions. With regard to the line strengths for the various overtones, the Benedict, Plyler and Humphreys predictions (*28*) are still in

[5] Both the Hönl–London and the Benedict, Plyler and Humphreys expressions are summed over the initial rotational state degeneracies and correspond to $(2J' + 1)S_{J',J''}$.

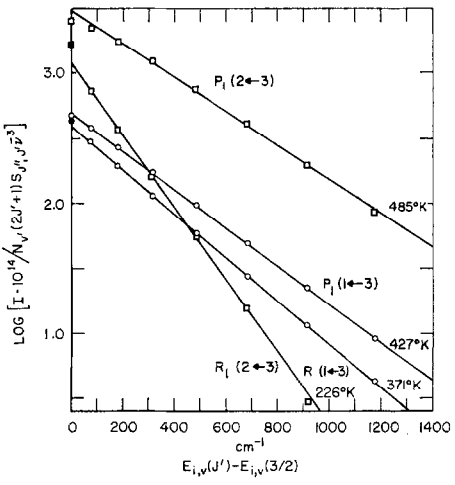

FIG. 4. Anomolous rotational temperatures. The exact rotational line intensities, I, are calculated at 400 K. The Benedict, Plyler, and Humphreys (*28*) rotational line strengths, $S_{J'',J'}$, are then used to determine the 'apparent' rotational temperatures that are shown for the P_1 and R_1 branches of the $2 \leftarrow 3$ (open squares) and the $1 \leftarrow 3$ (open circles) vibrational bands.

error (especially for high v'), but to a less significant degree than for the fundamentals. Using improper linestrengths introduces an implicit J' dependence in $C(v'' \leftarrow v')$ in Eq. (43) which is then dependent on $E_{i',v'}(J')$ and contributes to the slope such that it no longer equals $1/kT_{\text{rot}}$. Such effects can give rise to *apparent* differences in the rotational temperatures determined from, say, the P and R branches of a given band, or the temperatures determined from two different bands originating from the same initial v' state [see (*3*), (*5*) and (*11*)]. A more subtle effect is that it can lead to apparent anomalies in the temperatures of the two multiplet states $i' = 1, 2$ (*30*).

An interesting demonstration of these errors in interpretation is given in Fig. 4. The exact theoretical Einstein coefficients were used in Eq. (41) to determine $I/N_{v'}$ for a Boltzmann distribution of multiplet-rotational states at exactly 400 K. The Benedict, Plyler and Humphreys (*28*) linestrengths for OH were then employed in Eq. (43) to determine rotational temperatures from the P_1 and R_1 branches of the $2 \leftarrow 3$ and $1 \leftarrow 3$ bands. The overtone band predicts a false temperature of 427 K for the P_1 branch and 371 K for the R_1 branch. The fundamental band predicts a temperature of about 500 K for the P_1 branch and 226 K for the weak R_1 branch. Obviously the exact Einstein coefficients that are tabulated in Appendix C for each specific multiplet-rotational line must be used in Eq. (41) if accurate rotational temperatures are required.

C. Thermally Averaged Vibrational Band Intensities and Integrated Absorption Coefficients

The relative intensities of series of Δv transitions ranging from the fundamentals $\Delta v = 1$ to $\Delta v = 7$, for various initial v' states have been measured under a wide range of conditions, with varying and often poor degrees of accuracy and resolution. These measurements range from atmospheric observations (*2, 3, 4*) with $T_{\text{rot}} \approx 200$ K, to H + O_3 flow systems (*5, 6, 11, 31*) with $T_{\text{rot}} \approx 500$ K, to OH emission in oxyacetylene flames (*28, 32*) with $T_{\text{rot}} \approx 2500$ K. The theoretically derived absolute emission rate

Table VI; Thermally Averaged Einstein Coefficients $A_{v''\leftarrow v'}(T)$ sec^{-1}

v'		v'' = v'-1	v'-2	v'-3	v'-4	v'-5	v'-6	Total
1	200°K	20.15						20.15
	500°K	20.00						20.00
	2500°K	19.39						19.39
2	200°K	25.24	14.07					39.31
	500°K	25.23	13.98					39.21
	2500°K	25.89	13.37					39.25
3	200°K	20.90	39.93	0.920				61.75
	500°K	21.35	39.63	0.913				61.89
	2500°K	25.12	37.56	0.870				63.55
4	200°K	12.25	72.61	4.29	0.079			89.23
	500°K	13.47	72.02	4.27	0.075			89.84
	2500°K	22.19	68.01	4.09	0.060			94.35
5	200°K	4.47	108.4	10.62	0.392	0.050		124.0
	500°K	6.79	107.4	10.56	0.390	0.047		125.2
	2500°K	22.08	100.7	10.12	0.374	0.033		133.4
6	200°K	2.347	141.5	20.99	1.274	0.053		166.3
	500°K	6.026	139.9	20.88	1.266	0.052		168.2
	2500°K	28.89	126.5	20.13	1.208	0.047		176.9
7	200°K	9.142	163.4	37.32	2.907	0.183		213.0
	500°K	14.32	161.0	37.18	2.881	0.183		215.7
	2500°K	44.71	146.5	36.04	2.721	0.182		229.8
8	200°K	25.84	166.8	60.84	5.67	0.569	0.030	259.8
	500°K	32.41	163.7	60.62	5.64	0.556	0.030	263.0
	2500°K	68.70	145.4	58.59	5.44	0.533	0.029	278.7
9	200°K	50.65	146.6	90.28	10.81	1.189	0.130	299.7
	500°K	58.12	143.1	89.86	10.81	1.177	0.132	303.3
	2500°K	96.79	123.8	85.93	10.75	1.101	0.137	318.5

constants, calculated from Eq. (38), are tabulated in Table VI for these three representative temperatures. These calculations include the contribution of the satellite bands to $A_{v''\leftarrow v'}(T)$, but they do not significantly contribute to the summation, and Table VI

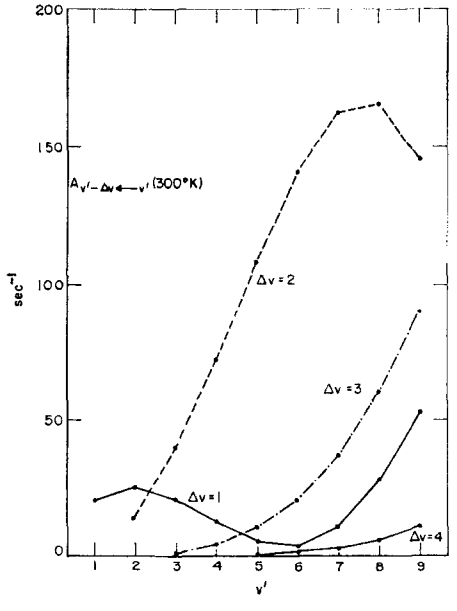

FIG. 5. Boltzmann averaged Einstein coefficients (Eq. 28) for the vibrational bands $v' - \Delta v \leftarrow v'$ at 300 K.

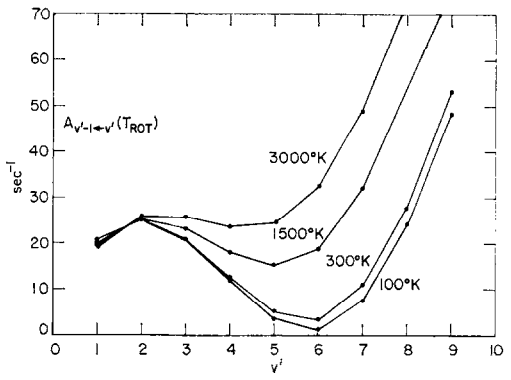

FIG. 6. Temperature dependence of the Boltzmann averaged Einstein coefficients for the fundamental transitions $A_{v'-1\leftarrow v'}(T_{\text{rot}})$. The variation with temperature is caused by rotation–vibration coupling.

can be generated entirely from the data in Appendix C. A plot of the rate constants vs v' at $T_{\text{rot}} = 300$ K is shown in Fig. 5, and demonstrates the significant amount of emission that originates in the OH overtone bands.

A comparison between theory and experiment is difficult because the experimental observations can only give accurate values for the ratios of different Δv transitions originating from the same initial state v'. In addition, Eq. (42) is generally employed, and, as discussed above, improper linestrengths are used to reduce the data and obtain a measure of the vibrational band strength $P_{v''\leftarrow v'}$. A more significant complication is introduced by the large vibration–rotation interactions which are generally ignored by setting $F = 1$. An indirect measure of these effects is indicated by the temperature dependence of $A_{v''\leftarrow v'}(T)$, particularly for $\Delta v = 1$, which is plotted in Fig. 6.

Garvin (*5*) has measured the relative intensities of the higher overtones using specific rotational lines and derived relative band strengths $P_{v''\leftarrow v'}$ from Eq. (42). He has been careful to average the appropriate P and R lines to minimize the effect of the factor F, which can then be ignored to first order in the vibration–rotation coupling. Multiplying

Table VII. Comparison of Theoretical and Experimental $A_{v'-\Delta v\leftarrow v'}$

v'	Δv=1	Δv=2	Δv=3	Δv=4	Δv=5	Δv=6	Δv=7
9	50.7	147	90.3	10.8	1.19	0.130	.
		356	90.3	12.4	0.61	0.112	.024
				10.8	1.44	0.336	~.04
8	25.8	166	60.8	5.67	0.570		
		341	60.8	7.67	0.51	0.075	
				5.67	0.76	0.11	
7	9.14	164	37.3	2.91	0.183		
		244	37.3	3.39	0.151	0.020	
			37.3	4.2	0.37	0.042	
6	2.35	142	21.0	1.27	0.053		
		162	21.0	0.92	0.036	0.003	
			21.0	1.8	0.15	0.007	
5	4.48	108	10.6	0.39			
		123	10.6	0.16	0.006		
			10.6	0.80	0.031		
4	12.3	73	4.29	~0.08			
		61	4.29	0.02			
			4.29	0.18			

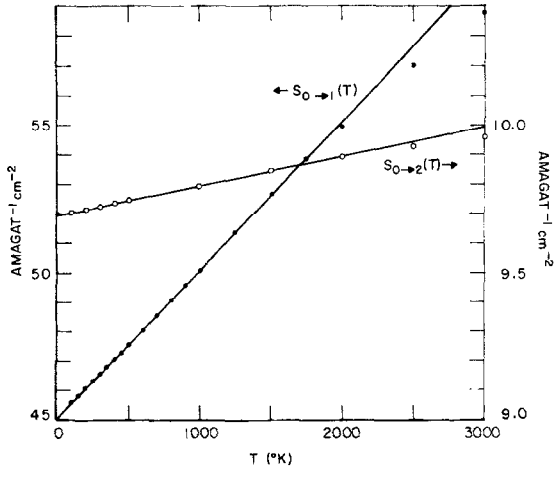

FIG. 7. Temperature dependence of the thermally averaged integrated absorption coefficients for the transitions $0 \rightarrow 1$ and $0 \rightarrow 2$.

Garvin's bandstrengths by ω^3 we can compare his relative values to the theoretical rate constants, $A_{v'',v'}(200\text{ K})$ in Table VI. This comparison is shown in Table VII. The theoretical data results are also compared to the relative band intensities of the overtones measured in the OH airglow which have been presented by Krassovsky *et al.* (*4*). Both sets of experimental results have been normalized for each v' state to the theoretical data at the underscored data entries. The overall agreement is satisfactory considering the degree of uncertainty in both experiment and theory.

The thermally averaged integrated absorption coefficient $S_{v''\leftarrow v'}(T)$ is plotted against temperature in Fig. 7, for the $0 \rightarrow 1$ and $0 \rightarrow 2$ bands. There is no absorption data available with which to compare these results.

D. The Absolute Intensities of the OH Vibrational Bands

Probably the most useful feature of the theoretical calculations is that we obtain the *absolute* magnitude of the Einstein coefficients $A_{v''\leftarrow v'}(T)$ in Eq. (38). The total number of photons emitted in the vibrational band $v'' \leftarrow v'$ per sec per cm^3 of emitting gas, $I_{v''\leftarrow v'}(T)$, assuming a Boltzmann distribution of multiplet-rotational states i', J', is obtained by summing Eq. (41), and yields

$$I_{v''\leftarrow v'}(T_{\text{rot}}) = N_{v'} A_{v''\leftarrow v'}(T_{\text{rot}}). \tag{44}$$

The Einstein coefficients are, of course, very difficult to obtain experimentally, especially for a vibrationally excited radical, and the rate constants in Table VI can now be used to determine the absolute OH concentrations $N_{v'}$ in both atmospheric and laboratory experiments.

Benedict and Plyler (*29*) have estimated the $0 \leftarrow 2$ integrated absorption coefficient to be 4 cm^{-2} Amagat^{-1} based on the assumption of thermodynamic equilibrium between various radicals in their emission spectra. This converts to an Einstein coefficient of 5.4 sec^{-1} compared to our calculated value of 13.4 sec^{-1} at 2500 K. They also quote an Einstein coefficient of 33 sec^{-1} for $0 \leftarrow 1$, although this transition was not measured in

their experimental spectra and must be a ball park estimate. The theoretical value for $0 \leftarrow 1$ is 20 sec^{-1}.

Potter *et al.* (*31*) have measured the OH($v' = 9$) afterglow in a H + O_3 flow system and on the basis of various kinetic arguments obtain a total radiative decay rate of 16 sec^{-1} for the $v' = 9$ state. This disagrees markedly with the theoretical value of 300 sec^{-1} which is given in Table VI. The discrepancy is difficult to resolve since the experimental observations are not a direct measure of the lifetime, but are dependent on the mechanism one chooses to interpret, and extrapolate (twice) the data. It must be conceded that our confidence in the theoretical results decreases with increasing v', but it is difficult to imagine any improvements in the theory which could change the $v' = 9$ decay rate by a factor of 20. As shown in Table IV, the theoretical transition moment matrix elements for $v' = 9$ were not especially sensitive to the improvement in the theoretical dipole moment function, and a discrepancy of that magnitude is inconsistent with Table VII where the theoretical ratios are in fair agreement with the experimental ratios for the overtone intensities.

The absolute intensity of the $0 \leftarrow 1$ and $1 \leftarrow 2$ emission bands has been measured by d'Incan *et al.* (*32*) in an oxyacetylene flame experiment. An equilibrium concentration of OH and distribution of excited vibrational levels is calculated, based on an unspecified determination of the P-branch rotational temperature, and the transition dipole matrix elements for these transitions is obtained. Their results predict $A_{0\leftarrow 1} \approx 8.5$ sec^{-1} and $A_{1\leftarrow 2} \approx 13$ sec^{-1}, as compared to 20 sec^{-1} and 25 sec^{-1} calculated theoretically. One possible explanation of the discrepancy might be an error in the estimated experimental temperature. As discussed above, and shown in Fig. 4, improper analysis of the rotation–vibration coupling causes an overestimate of the true temperature in the P branch of the fundamental transitions (for $v' < 6$). This would probably lead to an overestimate of the excited state concentration, and an underestimate of the radiative transition rates.

VII. SUMMARY AND CONCLUSIONS

The vibrational–rotational transition probabilities for OH($X^2\Pi$) have been calculated using the theoretically derived dipole moment, $d(R)$, published by Stevens *et al.* (*10*) which is shown in Fig. 1. The present calculations take full and accurate account of the intermediate spin uncoupling in the $^2\Pi$ rotational–electronic states and the vibrational–rotational coupling caused by centrifugal distortion. Numerically derived RKR vibrational wavefunctions are used, and the ultimate accuracy of the calculated intensities is determined solely by the accuracy of the function $d(R)$, which is used to evaluate the vibrational transition matrix elements, $R_{v',v''} = \langle v' | d(R) | v'' \rangle$. The accuracy of $d(R)$ is best discussed in terms of the following expression,

$$d(R) = d(R_e) + \lambda f(R - R_e), \tag{45}$$

where $f(0) = 0$. The completeness of the electronic wavefunction used to calculate $d(R)$ is discussed by Stevens *et al.* (*10*), and judged by the excellent agreement between the theoretical and experimental dipole moment for the $v = 0$ state, i.e., $\langle 0 | d(R) | 0 \rangle$, which is determined primarily by $d(R_e)$, the accuracy of $d(R_e)$ is about 1%. Unfortunately, the vibrational transition probabilities are insensitive to $d(R_e)$, and are deter-

mined by λf. Small changes in the functional dependence of $f(R - R_e)$ can cause very sensitive changes in certain of the transition matrix elements, as is shown in Table IV and Fig. 2. However, except for the lifetime of the $v' = 9$ state, which disagrees markedly with the estimate deduced by Potter *et al.* (*31*), the theoretical predictions are consistent with a variety of often very imprecise experimental data, which suggests that λf can not be in serious error, and the predicted absolute intensities, especially for $\Delta v = 2$, are reliable. The following results and conclusions have been obtained.

(i) The intensity of the first overtone, $\Delta v = 2$, is generally larger than the fundamental intensities. This result confirms the measurements of Murphy (*11*) and substantiates the general shape of the function $f(R - R_e)$ in the vicinity of R_e. The ratios of various overtone intensities originating from the same initial vibrational level v' generally agree with experimental observations, and suggest that the functional dependence of $f(R - R_e)$ is correct for all R. However, these relative intensities are independent of the scaling parameter λ.

(ii) There is very strong rotational–vibrational coupling in OH, which causes the P and R branch intensities, especially in the fundamental bands, to vary markedly with v'. The exceptionally good agreement between theory and Murphy's experimental linestrengths, implies that the ratio $\lambda f(R - R_e)/d(R_e)$ is accurate, at least for $R \approx R_e$. Since $d(R_e)$ is known to be correct to within 1%, then λf, and hence the scaling parameter λ, must also be given accurately by the theoretical function $d(R)$, and therefore the calculations should yield reliable values for the *absolute* intensities.

(iii) The fact that the spin-uncoupling and vibrational–rotational coupling is large causes the rotational linestrengths to differ significantly from Hönl–London or Benedict, Plyler and Humphrey's values (*28*), and the rotational temperatures one derives with these improper linestrengths are often in significant error. The correct linestrengths are tabulated in Appendix C.

(iv) The Boltzmann averaged vibrational band intensities for $v' = 1, 9$ and $v = 1, 5$ are presented for several temperatures. The absolute values of these transition rate constants should yield reliable estimates of OH(v') concentrations from experimental intensity measurements. Complete certainty in the theoretical results must await either more accurate experimental confirmation, or more precise error limits on the theoretical dipole moment function, $d(R)$.

APPENDIX A. ANALYSIS OF LAMBDA DOUBLING EFFECTS

We have ignored the coupling of the $|J, M, P; {}^2\Pi_\Omega\rangle$ state to the $|J, M, P; {}^2\Sigma_{\frac{1}{2}}^+\rangle$ state in solving the set of coupled equations (5) and (6). We will now examine the influence of this coupling on the approximate solutions $|J, M, P; \alpha\rangle$ that are defined in Eq. (26).[6]

$$|J, M, P; \alpha\rangle = \sum_{\Omega, v_0} \mathcal{C}_{v_0, \alpha}^{\Omega} |\Omega, v_0\rangle \tag{A.1}$$

where

$$|\Omega, v_0\rangle \equiv |J, M, P; {}^2\Pi_\Omega\rangle |v_0\rangle. \tag{A.2}$$

[6] A study of this effect on the $A \rightarrow X$ transition in OH has been presented by German, *et al.* (*35*).

Let

$$|0, \eta\rangle \equiv |J, M, P; {}^2\Sigma_{\frac{1}{2}}^+\rangle|\eta\rangle \tag{A.3}$$

where $|\eta\rangle$ is the vibrational wavefunction for the "unperturbed" ${}^2\Sigma_{\frac{1}{2}}^+$ state obtained from solving Eq. (7) with $F_\Omega(R) = 0$, i.e.,

$$\langle {}^2\Sigma_{\frac{1}{2}}^+|H - E_{J,\eta}|{}^2\Sigma_{\frac{1}{2}}^+\rangle|\eta\rangle = 0 \tag{A.4}$$

($|{}^2\Sigma_{\frac{1}{2}}^+\rangle$ is an abbreviated notation for the rotational electronic wavefunction $|J, M, P; {}^2\Sigma_{\frac{1}{2}}^+\rangle$). Using first-order perturbation theory to estimate the contribution of the $G^+(R)$ term in Eq. (1), we obtain the following perturbation result for Eq. (A.1),

$$|J, M, P; \alpha\rangle^{\text{pert}} \approx \sum_{\Omega, v_0} \mathcal{A}_{v_0,\alpha}{}^{\Omega}\left\{|\Omega, v_0\rangle + \sum_{\eta} \frac{\langle \Omega, v_0|H|0, \eta\rangle}{E_{J,\alpha} - E_{J,\eta}}|0, \eta\rangle\right\}. \tag{A.5}$$

Due to this admixture of ${}^2\Sigma^+$ state the bracketed term $\{R_{v_0', v_0''}\delta_{\Omega',\Omega''}\} \equiv T_{\Omega',\Omega''}(v_0', v_0'')$ in the intensity expression (36) must be modified. Let

$$\begin{aligned} M_x(R) &= \langle {}^2\Sigma^+, \Lambda = 0, \Sigma|m_1|{}^2\Pi, \Lambda = -1, \Sigma\rangle \\ &= -\langle {}^2\Pi, \Lambda = 1, \Sigma|m_1|{}^2\Sigma^+, \Lambda = 0, \Sigma\rangle, \end{aligned} \tag{A.6}$$

where

$$m_1 = -e\sum_j (-x_j - iy_j)2^{-\frac{1}{2}}.$$

This is the transition dipole moment function for the $A \rightarrow X$ transition of OH, where x_j and y_j are the molecule-fixed coordinates of the jth electron. $M_x(R)$ is equivalent to the matrix element $\langle {}^2\Sigma^+|x|{}^2\Pi_x\rangle$ calculated by Henneker and Popkie [33], and we shall employ the values tabulated in Table IV of their paper. An excellent linear fit is obtained with $M_x(R) = 0.4006 - 0.1514\ R$, in atomic units.

We define the following series,

$$B^{\pm} = \sum_{\eta} \frac{\langle v_0'|B\bar{L}|\eta\rangle\langle\eta|M_x|v_0''\rangle}{E_{J',\eta} - E_{J',\alpha'}} \pm \frac{\langle v_0'|M_x|\eta\rangle\langle\eta|B\bar{L}|v_0''\rangle}{E_{J'',\eta} - E_{J'',\alpha''}}, \tag{A.7}$$

$$A^{\pm} = \sum_{\eta} \frac{\langle v_0'|\frac{A_{\Sigma\Pi}}{2}|\eta\rangle\langle\eta|M_x|v_0''\rangle}{E_{J',\eta} - E_{J',\alpha'}} \pm \frac{\langle v_0'|M_x|\eta\rangle\langle\eta|\frac{A_{\Sigma\Pi}}{2}|v_0''\rangle}{E_{J'',\eta} - E_{J'',\alpha''}}, \tag{A.8}$$

and

$$S^{\pm} = A^{\pm} + B^{\pm}. \tag{A.9}$$

$B\bar{L}$ and $A_{\Sigma\Pi}$ are the R-dependent terms defined in Eqs. (11), (19) and (15). Great care must be taken to insure that the electronic elements M_x, $B\bar{L}$ and $A_{\Sigma\Pi}$ are all evaluated with the *same* electronic wavefunctions to obtain the proper phase relationships between the elements. This holds true for the vibrational matrix elements as well.

With these definitions the perturbed amplitude (36) may be expressed as follows

$$\mathcal{P} = \tfrac{1}{2}[1 - P'P'']\sum_{\Omega',\Omega'',v_0',v_0''} \mathcal{A}_{v_0',\alpha'}{}^{\Omega'*}\mathcal{A}_{v_0'',\alpha''}{}^{\Omega''} \times C(J', 1, J''; \Omega', \Omega'' - \Omega', \Omega'')T_{\Omega',\Omega''}, \tag{A.10}$$

Table A.I: $C(J',1,J''|\Omega',\Omega''-\Omega',\Omega'')T_{\Omega',\Omega''}$

		$\Omega''=3/2$	$\Omega''=1/2$
$\Omega'=3/2$	$J''=J'+1$	$\sqrt{\frac{(J'-1/2)(J'+5/2)}{(2J'+1)(2J'+2)}}\cdot\left\{\sqrt{2}\,R_{v_0',v_0''}-\frac{B^+}{2}-(J'+1)B^-\right\}$	$\sqrt{\frac{(J'-1/2)(J'+1/2)}{(2J'+1)(2J'+2)}}\cdot\left\{-\frac{S^+}{2}+\frac{S^-}{2}-\Pi'(J'+3/2)B^-\right\}$
	$J''=J'$	$\sqrt{\frac{1}{2J'(J'+1)}}\cdot\left\{R_{v_0',v_0''}\frac{3}{\sqrt{2}}+(J'-1/2)(J'+3/2)B^+\right\}$	$\sqrt{\frac{(J'-1/2)(J'+3/2)}{2J'(J'+1)}}\cdot\left\{-\frac{S^+}{2}+\frac{S^-}{2}+\Pi'(J'+1/2)B^-\right\}$
	$J''=J'-1$	$\sqrt{\frac{(J'-3/2)(J'+3/2)}{2J'(2J'+1)}}\cdot\left\{-\sqrt{2}R_{v_0',v_0''}+\frac{B^+}{2}-J'B^-\right\}$	$\sqrt{\frac{(J'+3/2)(J'+1/2)}{2J'(2J'+1)}}\cdot\left\{-\frac{S^+}{2}+\frac{S^-}{2}-\Pi'(J'+1/2)B^-\right\}$
$\Omega'=1/2$	$J''=J'+1$	$\sqrt{\frac{(J'+3/2)(J'+5/2)}{(2J'+1)(2J'+2)}}\cdot\left\{\frac{S^+}{2}+\frac{S^-}{2}-\Pi'(J'+1/2)B^-\right\}$	$\sqrt{\frac{(J'+1/2)(J'+3/2)}{(2J'+1)(2J'+2)}}\cdot\left\{\sqrt{2}R_{v_0',v_0''}+\Pi'S^-+\frac{B^+}{2}-(J'+1)B^-\right\}$
	$J''=J'+1$	$\sqrt{\frac{(J'-1/2)(J'+3/2)}{2J'(J'+1)}}\cdot\left\{-\frac{S^+}{2}-\frac{S^-}{2}+\Pi'(J'+1/2)B^-\right\}$	$\sqrt{\frac{1}{2J'(J'+1)}}\cdot\left\{R_{v_0',v_0''}\frac{1}{\sqrt{2}}-\Pi'(J'+1/2)S^-+(J'+1/2)^2B^+\right\}$
	$J''=J'-1$	$\sqrt{\frac{(J'-3/2)(J'-1/2)}{2J'(2J'+1)}}\cdot\left\{\frac{S^+}{2}+\frac{S^-}{2}-\Pi'(J'+1/2)B^-\right\}$	$\sqrt{\frac{(J'-1/2)(J'+1/2)}{2J'(2J'+1)}}\cdot\left\{-\sqrt{2}R_{v_0',v_0''}+\Pi'S^--\frac{B^+}{2}-J'B^-\right\}$

where

$$T_{\Omega',\Omega''}=\left\{R_{v_0',v_0''}+\frac{1}{\sqrt{2}}\left[\delta_{J',J''}\frac{J'(J'+1)}{\Omega}+(1-\Omega)\right]B^+\right.$$

$$+\left[J'(J'+1)-J''(J''+1)\right]\frac{B^-}{2\sqrt{2}}-\left[\Pi'(J'+\tfrac{1}{2})-\Pi''(J''+\tfrac{1}{2})\right]$$

$$\left.\times\frac{S^-}{\sqrt{2}}\delta_{\Omega',\frac{1}{2}}\right\}\delta_{\Omega',\Omega''}+(\Omega'-\Omega'')\left[\frac{S^+}{2}-\delta_{\Omega',\frac{1}{2}}\delta_{\Omega'',\frac{3}{2}}\left[\frac{S^-}{2}+\Pi'(J'+\tfrac{1}{2})B^-\right]\right.$$

$$\left.-\delta_{\Omega',\frac{3}{2}}\delta_{\Omega'',\frac{1}{2}}\left[\frac{S^-}{2}+\Pi''(J''+\tfrac{1}{2})B^-\right]\right]. \quad \text{(A.11)}$$

Explicit expressions for $C(J',1,J''|\Omega',\Omega''-\Omega',\Omega'')T_{\Omega',\Omega''}$ are given in Table A.I. Some of the terms involving B^- and S^- are multiplied by the phase factor $\Pi = Pe^{i\pi(J-\frac{1}{2})}$ and gives rise to differences in the perturbed intensities for the pair of Λ-doublet states with $P=\pm 1$.

Not surprisingly the influence of the Λ-doubling effect increases with J'. The most marked effect occurs in the Q-branch intensities where we get contributions of the order J^2B^+ and J^2B^- relative to the unperturbed $R_{v_0',v_0''}$ transition matrix element. For the P and R branches the B^+ contribution is negligible and the dominant terms, relative to $R_{v_0',v_0''}$, involve JB^-. Estimates of these terms must be obtained.

Simplified expressions can be derived for Eqs. (A.7) and (A.8) by noting the following equality (*34*, Chap. VII).

$$\mathcal{O}^{\pm}=\sum_{\eta}\frac{\langle v_0'|\mathcal{O}|\eta\rangle\langle\eta|M_x|v_0''\rangle}{E_{J',\eta}-E_{J',\alpha'}}\pm\frac{\langle v_0'|M_x|\eta\rangle\langle\eta|\mathcal{O}|v_0''\rangle}{E_{J'',\eta}-E_{J'',\alpha''}},$$

$$\equiv\langle v_0'|Q_{\pm}|v_0''\rangle, \quad \text{(A.12)}$$

where

$$Q_{\pm}=\mathcal{O}(1/H_{\Sigma,J'}-E_{J',\alpha'})M_x\pm M_x(1/H_{\Sigma,J''}-E_{J'',\alpha''})\mathcal{O}. \quad \text{(A.13)}$$

The Hamiltonian $H_{\Sigma,J}(R) \equiv \langle J, M, P, {}^2\Sigma_{\frac{1}{2}}^+ | H | J, M, P, {}^2\Sigma_{\frac{1}{2}}^+ \rangle$ is the vibrational Hamiltonian for the ${}^2\Sigma_{\frac{1}{2}}^+$ state which appears in Eq. (A.4) and is defined in Table I. We can express the operator in terms of the Hamiltonian $H_{\Pi,J_0} \equiv T_R + B(R)J_0(J_0+1) + W_\Pi{}^{\text{eff}}(R)$ in Eq. (20) which in turn defines the approximate set of ${}^2\Pi$ vibrational wavefunctions $|v_0\rangle$ and eigenvalues $E_{v_0}{}^0$,

$$H_{\Sigma,J} = H_{\Pi,J_0} + \Delta W(R), \tag{A.14}$$

$$\Delta W \equiv W_\Sigma{}^{\text{eff}}(R) - W_\Pi{}^{\text{eff}}(R) + B(R)\{(J-\tfrac{1}{2})(J+\tfrac{1}{2}) + 1 - \Pi(J+\tfrac{1}{2}) - J_0(J_0+1)\} \approx W_\Sigma{}^{\text{eff}}(R) - W_\Pi{}^{\text{eff}}(R). \tag{A.15}$$

The resolvent $1/(H_{\Sigma,J} - E_{J,\alpha})$ can be expanded in powers of $\epsilon/\Delta W$, where $\epsilon = E_{J,\alpha} - H_{\Pi,J_0}$,

$$\frac{1}{H_{\Sigma,J} - E_{J,\alpha}} \approx \frac{1}{\Delta W} + \frac{1}{\Delta W}\epsilon\frac{1}{\Delta W} + \frac{1}{\Delta W}\epsilon\frac{1}{\Delta W}\epsilon\frac{1}{\Delta W} + \cdots.$$

The leading term for $\mathcal{O}^+$ is then,

$$\mathcal{O}^+ = \langle v_0' | 2M_x\mathcal{O}/\Delta W | v_0'' \rangle. \tag{A.16}$$

Eqs. (A.7), (A.8) and (A.9) can then be approximated as follows,

$$B^+ \approx \langle v_0' | 2M_x B\bar{L}/\Delta W | v_0'' \rangle, \tag{A.17}$$

$$S^+ \approx \langle v_0' | (2M_x/\Delta W)[B\bar{L} + (A_{\Sigma\Pi}/2)] | v_0'' \rangle. \tag{A.18}$$

We will ignore the R-dependence of ΔW and assume $\Delta W \approx T_e \equiv 32\,682\ \text{cm}^{-1}$. The matrix elements $\langle v_0' | M_x B\bar{L} | v_0'' \rangle$ and $\langle v_0' | M_x(B\bar{L} + A_{\Sigma\Pi}/2) | v_0'' \rangle$ have been evaluated numerically using Morse functions to represent the ${}^2\Pi$ vibrational wavefunctions $|v_0\rangle$. These values are tabulated in Table AII.

Approximating $E_{v_0'}{}^0 - E_{v_0''}{}^0 \approx E_{J',\alpha'} - E_{J'',\alpha''}$, the leading term for $\mathcal{O}^-$, to second order in $(1/\Delta W)$, is

$$\mathcal{O}^- \approx \langle v_0' | \int dR \frac{2M_x}{\Delta W^2}\frac{d\mathcal{O}}{dR} | v_0'' \rangle (E_{v_0'}{}^0 - E_{v_0''}{}^0).$$

Since we assume $dA_{\Sigma\Pi}/dR \approx 0$, we obtain the result $A^- \approx 0$ and $S^- \approx B^-$ from Eqs. (A.8) and (A.9). Again equating $\Delta W \approx T_e$, we obtain the following result for B^-.

$$B^- \approx S^- \approx \langle v_0' | \int dR 2M_x \frac{dB\bar{L}}{dR} | v_0'' \rangle (E_{v_0'}{}^0 - E_{v_0''}{}^0)/T_e{}^2. \tag{A.19}$$

Recalling that $B = \hbar^2/(2\mu R^2)$, $M_x = 0.4006 - 0.1514R$, and assuming $\bar{L} \neq fcn(R)$, the integral in (A.19) may be expressed as follows.

$$\langle v_0' | \int dR 2M_x \frac{dB\bar{L}}{dR} | v_0'' \rangle = 4\langle v_0' | M_x B\bar{L} | v_0'' \rangle - 0.8012\bar{L}\langle v_0' | B | v_0'' \rangle.$$

$\langle v_0' | M_x B\bar{L} | v_0'' \rangle$ is given in Table AII, and $\langle v_0' | B | v_0'' \rangle$ is listed in Table III. Some representative values of $R_{v_0',v_0''}$, B^+, B^-, S^+ and S^- are presented in Table A.III.

An examination of the intensity expressions in Table A.I, using the numerical results in Table A.III, leads to the conclusion that the ${}^2\Sigma_{\frac{1}{2}}^+$ contributions to the Meinel band

Table A.II: Matrix elements (cm^{-1} x a.u.) at $\langle v_o' | \bar{BL} M_x | v_o'' \rangle$ and $\langle v_o' | (\bar{BL} + \frac{1}{2}A_{\Delta\Gamma}) M_x | v_o'' \rangle$

v_o'' \ v_o'	0	1	2	3	4	5	6	7	8	9
0	3.058 -6.270	0.9148 -0.6692	0.2586 0.0772	0.08796 0.05366	0.03413 0.02569	0.01480 0.01199	0.00696 0.00597	0.00353 0.00311	0.00194 0.00167	0.00109 0.00102
1		2.841 -5.699	1.227 -1.042	0.4254 0.1022	0.1674 0.09364	0.07284 0.05251	0.03450 0.02773	0.01757 0.01500	0.00956 0.00847	0.00551 0.00498
2			2.623 -5.075	1.422 -1.394	0.5693 0.0999	0.2506 0.1327	0.1198 0.08272	0.06151 0.04531	0.03361 0.02802	0.01946 0.01685
3				24.03 -4.397	1.548 -1.749	0.6930 0.0705	0.3350 0.1609	0.1734 0.11344	0.09536 0.07157	0.05546 0.04483
4					2.182 -3.654	1.626 -2.112	0.7977 0.0128	0.4170 0.1764	0.2312 0.1413	0.1352 0.09675
5						1.959 -2.837	1.666 -2.488	0.8828 -0.0729	0.4939 0.1761	0.2909 0.1632
6							1.735 -1.935	1.674 -2.881	0.9489 -0.1888	0.5635 0.1563
7								1.510 -0.934	1.656 -3.289	0.9953 -0.3347
8									1.284 +0.184	1.614 -3.714
9										1.057 +1.445

intensities, for say, $J \leqslant 20.5$, can generally be ignored. The dominant contribution to the P and R branches comes from JB^- which is approximately $\leqslant 0.05 |R_{v_0', v_0''}|$. The weaker Q-branch intensities can be significantly modified at high J since J^2B^+ becomes comparable to $R_{v_0', v_0''}$ in the range $J = 8.5 \leftrightarrow 20.5$. However, since the Q-branch intensities decrease rapidly ($1/J^2$) with increasing J, relative to the almost constant

Table A.III

$v_o' \to v_o''$	$R_{v_o', v_o''}$ x 10^5	B^+ x 10^5	B^- x 10^5	S^+ x 10^5	S^- x 10^5
1→0	-1410.	2.8	0.29	-2.0	0.29
2→1	-1671.	3.8	0.37	-3.2	0.37
3→2	-1592.	4.4	0.38	-4.3	0.38
4→3	-1224.	4.7	0.38	-5.4	0.38
5→4	- 578.	5.0	0.36	-6.5	0.36
6→5	+ 353.	5.1	0.33	-7.6	0.33
7→6	+1568.	5.1	0.28	-8.8	0.28
2→0	- 447.	0.79	0.21	+0.24	0.21
3→1	- 811.	1.3	0.32	+0.31	0.32
4→2	-1178.	1.7	0.41	+0.31	0.41
5→3	-1159.	2.1	0.47	+0.22	0.47
6→4	-1935.	2.4	0.48	+0.039	0.48
7→5	-2276.	2.7	0.50	-0.22	0.50
3→0	- 64.6	0.27	0.11	+0.16	0.11
4→1	- 151.	0.51	0.21	+0.29	0.21
5→2	- 256.	0.77	0.30	+0.41	0.30
6→3	- 390.	1.0	0.37	+0.49	0.37
7→4	- 567.	1.3	0.44	+0.54	0.44
4→0	- 13.7	0.10	0.061	+0.079	0.061
5→1	- 30.4	0.22	0.12	+0.16	0.12
6→2	- 59.8	0.37	0.20	+0.25	0.20
7→3	- 98.3	0.53	0.28	+0.35	0.28
5→0	- 7.3	0.045	0.033	+0.037	0.033
6→1	- 8.5	0.11	0.075	+0.085	0.075
7→2	- 16.7	0.19	0.13	+0.14	0.13

P- and R-branch intensities, these marked perturbations at large J are of no practical importance.

The above conclusions only apply to the strong P_{11}, Q_{11}, R_{11} and P_{22}, Q_{22}, R_{22} line intensities. However, the satellite lines P_{12}, Q_{12}, R_{12} and P_{21}, Q_{21}, R_{21} are generally weak because of significant cancellation effects which decrease the contribution of the $R_{v_0',v_0''}$ terms to the sum (A.10) by an order of magnitude, and the $^2\Sigma_{\frac{1}{2}}^+$ terms might play an important role in the intensities, especially in the Q branch.

APPENDIX B. TEST OF VIBRATIONAL EIGENFUNCTION EXPANSION

The secular equation (22) or (28) is nondiagonal predominantly because of the nondiagonal matrix $B_{v_0,v_0'}$

$$B_{v_0,v_0'} = \langle v_0 | \hbar^2/2\mu R^2 | v_0' \rangle. \tag{B.1}$$

The largest contribution occurs in the homogeneous term $\mathbf{S}$ or S, which is proportional to $J(J+1)\mathbf{B}$; this term produces vibrational–rotational coupling within a given state $i = 1, 2$. The inhomogeneous matrix $\mathcal{C}$ which couples the $i = 1$ and $i = 2$ set of HVV states has, by definition [see Eq. (30)], vanishing diagonal elements, and off-diagonal elements proportional to small differences in the coefficients $(\Phi_v - \Phi_{v'})$. Thus, a sufficient test of the expansions in (21) and (26) is the ability of a *truncated* set of vibrational eigenfunctions of (20), $|v_0\rangle$, obtained with some fixed value of J_0, to reproduce the *exact* solutions of (20), $|v\rangle$, with, say $J_0 = J$. Let

$$[T_R + W^{\text{eff}}(R) + J_0(J_0+1)B(R)]|v_0\rangle = E_{v_0}{}^0|v_0\rangle \tag{B.2}$$

and let

$$[T_R + W^{\text{eff}}(R) + J(J+1)B(R)]|v\rangle = E_v|v\rangle. \tag{B.3}$$

Since $|v_0\rangle$ forms a complete set we may expand the solutions $|v\rangle$ as follows,

$$|v\rangle = \sum_{v_0} C_{v_0,v}|v_0\rangle, \tag{B.4}$$

TABLE B.I

COMPARISON OF EXACT E_v AND TRUNCATED $\bar{E}_v$ EIGENVALUES

	$\bar{E}_v - E_v$ (cm^{-1})		
v	J=10, J_o=0	J=0, J_o=10	J=20, J_o=10
0	- 0.01	- 0.00	- 0.08
1	0.06	- 0.02	0.07
2	0.00	0.02	- 0.06
3	- 0.02	0.01	0.00
4	0.10	- 0.04	- 0.01
5	- 0.01	0.03	0.03
6	- 0.01	0.19	- 0.04
7	- 0.04	0.62	0.01
8	0.14	1.83	- 0.17
9	0.14	5.34	0.09
10	0.55	13.30	0.16
11	1.64	28.99	0.29

TABLE B.II

OVERLAP MATRIX $\langle v|t\rangle$ FOR J=10 AND J_o=0

t \ v	8[a]	9	10	11	12	13	14
0	0.00000	0.00001	-0.00000	-0.00000	-0.00000	-0.00000	-0.00000
1	-0.00000	0.00000	0.00000	0.00000	-0.00000	-0.00000	-0.00000
2	0.00000	-0.00000	0.00000	0.00000	0.00000	0.00000	-0.00000
3	0.00000	-0.00001	0.00000	0.00000	0.00000	0.00000	-0.00000
4	0.00001	-0.00000	-0.00000	-0.00000	-0.00000	-0.00001	-0.00001
5	-0.00001	-0.00000	-0.00001	-0.00000	-0.00000	-0.00001	-0.00002
6	-0.00001	0.00000	-0.00001	-0.00001	-0.00002	-0.00003	-0.00005
7	-0.00003	0.00001	-0.00002	-0.00003	-0.00004	-0.00007	-0.00013
8	1.00000	-0.00003	-0.00004	-0.00006	-0.00009	-0.00016	-0.00029
9	0.00005	0.99999	-0.00016	-0.00018	-0.00024	-0.00037	-0.00064
10	0.00004	0.00015	0.99997	0.00062	-0.00063	-0.00086	-0.00141
11	0.00005	0.00013	0.00048	0.99987	-0.00207	-0.00213	-0.00317
12	0.00004	0.00013	0.00039	0.00161	0.99953	-0.00691	-0.00778
13	0.00005	0.00015	0.00039	0.00121	0.00495	0.99783	-0.02474
14	0.00006	0.00015	0.00040	0.00112	0.00351	0.01497	0.98641
15	0.00015	0.00039	0.00099	0.00259	0.00720	0.02268	0.09219

(a) The off-diagonal matrix elements are all less than 0.00002 for $v \leq 7$

TABLE B.III

COMPARISON OF EXACT AND APPROXIMATE OVERLAP MATRICES FOR J=10, J_o=0

v	$C_{v-3,v}$	$C_{v-2,v}$	$C_{v-1,v}$	$C_{v,v}$	$C_{v+1,v}$	$C_{v+2,v}$	$C_{v+3,v}$
0				0.996835(a)	-0.079228	-0.006055	-0.001122
				0.996833(b)	-0.079279	-0.006046	-0.001114
				1.000000(c)	-0.078972	-0.010365	-0.002298
1			0.078077	0.990507	-0.112641	-0.010437	-0.002218
			0.078080	0.990504	-0.112652	-0.010441	-0.002210
			0.078966	1.000000	-0.111724	-0.017844	-0.004540
2		0.014491	0.109272	0.984052	-0.138788	-0.014744	-0.003477
		0.014499	0.109276	0.984051	-0.138785	-0.014755	-0.003475
		0.010365	0.111728	1.000000	-0.137033	-0.025134	-0.007113
3	0.003806	0.024708	0.132557	0.977418	-0.161416	-0.019093	-0.004916
	0.003813	0.024705	0.132555	0.977416	-0.161466	-0.019080	-0.004914
	0.002298	0.017844	0.137035	1.000000	-0.158690	-0.032392	-0.010015
4	0.007464	0.034433	0.151762	0.970549	-0.182116	-0.023516	-0.006539
	0.007461	0.034439	0.151780	0.970542	-0.182114	-0.023518	-0.006541
	0.004541	0.025135	0.158695	1.000000	-0.178098	-0.039738	-0.013252
5	0.011574	0.043914	0.168373	0.963367	-0.201589	-0.028075	-0.008356
	0.011574	0.043912	0.168369	0.963367	-0.201580	-0.028076	-0.008360
	0.007113	0.032391	0.178099	1.000000	-0.196113	-0.047213	-0.016832
6	0.016119	0.053255	0.183127	0.955772	-0.220532	-0.032829	-0.010401
	0.016123	0.053250	0.183136	0.955774	-0.220516	-0.032847	-0.010408
	0.010015	0.039738	0.196114	1.000000	-0.213351	-0.054948	-0.020805
7	0.021098	0.062503	0.196649	0.947620	-0.239344	-0.037865	-0.012714
	0.021092	0.062507	0.196642	0.947619	-0.239391	-0.037877	-0.012734
	0.013251	0.047215	0.213350	1.000000	-0.230203	-0.063004	-0.025233
8	0.026464	0.071795	0.209200	0.938749	-0.258573	-0.043258	-0.015365
	0.026472	0.071806	0.209214	0.938715	-0.258643	-0.043308	-0.015427
	0.016833	0.054949	0.230203	1.000000	-0.247012	-0.071541	-0.030217
9	0.032308	0.081196	0.221048	0.928836	-0.278718	-0.049175	-0.018485
	0.032297	0.081181	0.221044	0.928765	-0.278941	-0.049344	-0.018663
	0.020806	0.063003	0.247006	1.000000	-0.264238	-0.080772	-0.035969

(a) exact; (b) truncated expansion; (c) first order perturbation theory

where

$$C_{v_0,v} = \langle v_0 | v \rangle. \tag{B.5}$$

In addition to satisfying Eq. (B.5), the expansion coefficients $C_{v_0,v}$ must be the eigenvectors of the following infinite-order secular equation,

$$(E_{v_0}^0 - E_v)C_{v_0,v} + [J(J+1) - J_0(J_0+1)] \sum_{v_0'} B_{v_0,v_0'} C_{v_0',v} = 0. \tag{B.6}$$

We define $|t\rangle$, $\bar{E}_t$, and $\bar{C}_{v_0,t}$ as the solutions of a *truncated* basis,

$$|t\rangle = \sum_{v_0=0}^{N} C_{v_0,t} |v_0\rangle \tag{B.7}$$

which are obtained from a finite secular equation of the form (B.6) with $v_0' = 0, N$.

We wish to see how well approximate eigenfunctions $|t\rangle$ represent the first $N+1$ exact eigenfunctions $|v\rangle$. To do this we compare the eigenvalues E_v and $\bar{E}_v$, and we evaluate the overlap matrix $\langle v|t\rangle$

$$\begin{aligned} \langle v|t\rangle &= \sum_{v=0}^{N} \bar{C}_{v_0,t} \langle v|v_0\rangle \\ &= \sum_{v=0}^{N} \bar{C}_{v_0,t} C_{v_0,v}. \end{aligned} \tag{B.8}$$

This matrix should be equivalent to the unit matrix **1** if $|t\rangle$ is a "good" representation.

Tests were made for various combinations of J_0 and J, as follows. First we obtained exact, numerical solutions to both (B.2) and (B.3) using the RKR potential (*13*) for OH($X^2\Pi$) to represent $W^{\text{eff}}(R)$. Next we generated the matrix $B_{v_0,v_0'}(J_0)$ using the numerical solutions of (B.2), and the exact overlap matrix $C_{v_0,v} = \langle v_0|v\rangle$ between the two sets of solutions (B.2) and (B.3). The first 16 eigenfunctions generated by (B.2) were used to solve the secular equation (B.6) for the approximate eigenvalues $\bar{E}_t$ and the eigenvectors $\bar{C}_{v_0,t}$. Finally the overlap between the exact and approximate solutions were evaluated from (B.8) and deviations from the unit matrix were examined. Some typical results are presented in Tables B.I, B.II, and B.III which demonstrate the excellent agreement that is obtained between the exact wavefunctions and the truncated expansion for vibrational levels in the range 0–10.

Table B.I shows the deviations one may expect from the exact eigenvalues for various combinations of J_0 and J. Typically more accurate results are obtained for $J > J_0$ than for $J < J_0$. This is to be expected since for $J < J_0$ the expansion extends to higher v_0 values than for $J > J_0$ and the missing vibrational continuum contributions become more important. All the intensity calculations were performed with $J > J_0$ basis sets and with $|J - J_0| < 10$.

The overlap of the exact and the truncated wavefunctions is presented in Table B.II for the $J = 10$, $J_0 = 0$ solutions. Even for $v = 11$ where the approximate eigenvalue differs from the exact by 1.64 cm^{-1}, the error in the wavefunction is negligible with regard to calculating the intensities of the OH Meinel bands.

Table B.III is a tabulation of the overlap matrix $C_{v_0,v}$ between the $J_0 = 0$ and the $J = 10$ vibrational states. Three quantities are shown for each element; the exact numerical result; the truncated approximation which is in excellent agreement; and the first-order perturbation theory approximation. Obviously the two sets of vibrational states are nonorthogonal to a high degree. This is an indication that the vibrational–rotational coupling effects will play a very important role in the OH intensities.

APPENDIX C. TABLES OF CALCULATED EINSTEIN COEFFICIENTS

(This appendix consists of tables C.I, C.II, C.III, C.IV and CV).

Table C.I: Einstein Coefficients (sec^{-1}) for $\Delta v=1$ Transitions

v'	v''	J'	P_1	Q_1	R_1	P_2	Q_2	R_2
1	0	0.5	0.000	0.000	0.000	13.892	6.113	0.000
1	0	1.5	9.168	10.557	0.000	13.719	1.366	4.916
1	0	2.5	11.723	4.256	3.791	14.177	0.671	5.122
1	0	3.5	13.133	2.208	4.435	14.798	0.426	4.681
1	0	4.5	14.176	1.311	4.251	15.452	0.303	4.051
1	0	5.5	15.044	0.849	3.769	16.087	0.230	3.365
1	0	6.5	15.799	0.584	3.174	16.680	0.181	2.682
1	0	7.5	16.465	0.420	2.550	17.217	0.146	2.037
1	0	8.5	17.049	0.313	1.944	17.688	0.120	1.451
1	0	9.5	17.554	0.239	1.387	18.089	0.099	0.945
1	0	10.5	17.978	0.186	0.900	18.416	0.083	0.533
1	0	11.5	18.321	0.148	0.504	18.665	0.070	0.229
1	0	12.5	18.584	0.119	0.213	18.836	0.060	0.048
1	0	13.5	18.765	0.097	0.042	18.928	0.051	0.002
1	0	14.5	18.866	0.079	0.004	18.941	0.044	0.103
1	0	15.5	18.885	0.066	0.111	18.877	0.037	0.361
2	1	0.5	0.000	0.000	0.000	17.595	7.438	0.000
2	1	1.5	11.744	12.866	0.000	17.720	1.649	5.693
2	1	2.5	15.257	5.188	4.272	18.613	0.804	5.673
2	1	3.5	17.332	2.688	4.785	19.697	0.507	4.905
2	1	4.5	18.937	1.592	4.344	20.807	0.359	3.956
2	1	5.5	20.310	1.026	3.590	21.877	0.271	2.996
2	1	6.5	21.526	0.702	2.753	22.874	0.212	2.105
2	1	7.5	22.611	0.501	1.943	23.778	0.170	1.329
2	1	8.5	23.571	0.370	1.224	24.575	0.139	0.705
2	1	9.5	24.406	0.280	0.641	25.257	0.114	0.263
2	1	10.5	25.116	0.216	0.230	25.819	0.095	0.030
2	1	11.5	25.698	0.170	0.021	26.255	0.079	0.031
2	1	12.5	26.150	0.135	0.041	26.564	0.067	0.288
2	1	13.5	26.471	0.108	0.314	26.745	0.056	0.825
2	1	14.5	26.661	0.087	0.863	26.797	0.047	1.661
2	1	15.5	26.722	0.070	1.711	26.724	0.040	2.817
3	2	0.5	0.000	0.000	0.000	14.737	5.824	0.000
3	2	1.5	10.036	10.086	0.000	15.335	1.281	4.071
3	2	2.5	13.381	4.062	2.907	16.542	0.619	3.724
3	2	3.5	15.544	2.099	2.985	17.896	0.387	2.872
3	2	4.5	17.313	1.236	2.410	19.257	0.272	1.973
3	2	5.5	18.879	0.791	1.685	20.564	0.204	1.173
3	2	6.5	20.298	0.536	0.999	21.784	0.158	0.545
3	2	7.5	21.583	0.379	0.450	22.896	0.126	0.141
3	2	8.5	22.736	0.276	0.102	23.885	0.101	0.000
3	2	9.5	23.748	0.205	0.003	24.736	0.082	0.159
3	2	10.5	24.621	0.156	0.194	25.448	0.067	0.652
3	2	11.5	25.347	0.120	0.712	26.012	0.055	1.510
3	2	12.5	25.922	0.093	1.590	26.424	0.045	2.763
3	2	13.5	26.343	0.072	2.861	26.683	0.037	4.442
3	2	14.5	26.609	0.056	4.555	26.789	0.031	6.574
3	2	15.5	26.721	0.044	6.699	26.744	0.025	9.185
4	3	0.5	0.000	0.000	0.000	8.584	2.941	0.000
4	3	1.5	6.101	5.094	0.000	9.535	0.640	1.643
4	3	2.5	8.552	2.039	1.026	10.824	0.305	1.176
4	3	3.5	10.356	1.043	0.801	12.196	0.188	0.604
4	3	4.5	11.942	0.606	0.403	13.563	0.130	0.182
4	3	5.5	13.408	0.381	0.099	14.881	0.096	0.002
4	3	6.5	14.775	0.252	0.002	16.121	0.073	0.124
4	3	7.5	16.039	0.173	0.182	17.262	0.056	0.592
4	3	8.5	17.194	0.122	0.694	18.288	0.044	1.448
4	3	9.5	18.266	0.088	1.565	19.224	0.035	2.707
4	3	10.5	19.168	0.064	2.867	19.983	0.027	4.448
4	3	11.5	19.930	0.046	4.629	20.596	0.021	6.690
4	3	12.5	20.546	0.033	6.889	21.060	0.017	9.468
4	3	13.5	21.011	0.024	9.682	21.371	0.013	12.816
4	3	14.5	21.324	0.017	13.042	21.529	0.010	16.764
4	3	15.5	21.484	0.012	17.002	21.535	0.007	21.343

Table C.I - Continued

v'	v''	J'	P_1	Q_1	R_1	P_2	Q_2	R_2
5	4	0.5	0.000	0.000	0.000	2.652	0.556	0.000
5	4	1.5	2.138	0.957	0.000	3.538	0.118	0.082
5	4	2.5	3.414	0.371	0.008	4.569	0.054	0.001
5	4	3.5	4.570	0.181	0.040	5.660	0.032	0.175
5	4	4.5	5.701	0.099	0.304	6.768	0.021	0.683
5	4	5.5	6.816	0.057	0.880	7.860	0.014	1.576
5	4	6.5	7.902	0.034	1.820	8.909	0.010	2.896
5	4	7.5	8.942	0.020	3.176	9.895	0.007	4.686
5	4	8.5	9.918	0.012	4.991	10.799	0.004	6.986
5	4	9.5	10.811	0.006	7.310	11.605	0.003	9.837
5	4	10.5	11.611	0.003	10.176	12.304	0.002	13.277
5	4	11.5	12.303	0.001	13.628	12.886	0.001	17.344
5	4	12.5	12.880	0.000	17.706	13.343	0.000	22.073
5	4	13.5	13.333	0.000	22.444	13.672	0.000	27.499
5	4	14.5	13.659	0.000	27.877	13.872	0.000	33.649
5	4	15.5	13.856	0.001	34.035	13.942	0.000	40.552
6	5	0.5	0.000	0.000	0.000	0.002	0.177	0.000
6	5	1.5	0.052	0.318	0.000	0.157	0.041	0.805
6	5	2.5	0.271	0.145	1.001	0.504	0.021	1.847
6	5	3.5	0.636	0.087	2.194	0.983	0.015	3.284
6	5	4.5	1.112	0.062	3.723	1.551	0.012	5.168
6	5	5.5	1.668	0.048	5.661	2.174	0.011	7.539
6	5	6.5	2.275	0.040	8.064	2.821	0.010	10.440
6	5	7.5	2.905	0.036	10.981	3.467	0.010	13.911
6	5	8.5	3.536	0.033	14.461	4.090	0.010	17.992
6	5	9.5	4.145	0.032	18.549	4.672	0.010	22.724
6	5	10.5	4.715	0.031	23.281	5.197	0.011	28.140
6	5	11.5	5.230	0.030	28.699	5.654	0.011	34.278
6	5	12.5	5.678	0.031	34.836	6.032	0.012	41.166
6	5	13.5	6.050	0.031	41.724	6.326	0.013	48.833
6	5	14.5	6.338	0.032	49.391	6.531	0.014	57.299
6	5	15.5	6.538	0.032	57.857	6.647	0.014	66.582
7	6	0.5	0.000	0.000	0.000	2.934	2.872	0.000
7	6	1.5	1.285	5.068	0.000	1.556	0.629	4.756
7	6	2.5	0.900	2.144	4.732	0.769	0.307	7.741
7	6	3.5	0.478	1.179	8.151	0.309	0.197	10.910
7	6	4.5	0.186	0.748	11.543	0.073	0.145	14.508
7	6	5.5	0.034	0.520	15.248	0.000	0.116	18.626
7	6	6.5	0.002	0.387	19.415	0.046	0.097	23.323
7	6	7.5	0.068	0.304	24.129	0.175	0.085	28.644
7	6	8.5	0.206	0.248	29.452	0.359	0.076	34.631
7	6	9.5	0.391	0.209	35.434	0.574	0.070	41.323
7	6	10.5	0.606	0.182	42.114	0.801	0.065	48.745
7	6	11.5	0.830	0.161	49.525	1.023	0.061	56.925
7	6	12.5	1.048	0.146	57.693	1.228	0.058	65.881
7	6	13.5	1.249	0.134	66.637	1.405	0.056	75.624
7	6	14.5	1.422	0.125	76.369	1.547	0.055	86.159
7	6	15.5	1.561	0.118	86.894	1.650	0.053	97.483
8	7	0.5	0.000	0.000	0.000	12.244	8.894	0.000
8	7	1.5	6.361	15.681	0.000	8.578	1.925	12.042
8	7	2.5	6.009	6.575	11.220	6.272	0.921	17.666
8	7	3.5	4.921	3.569	17.813	4.608	0.580	22.862
8	7	4.5	3.833	2.224	23.505	3.357	0.419	28.314
8	7	5.5	2.892	1.516	29.194	2.406	0.327	34.225
8	7	6.5	2.120	1.102	35.212	1.688	0.269	40.691
8	7	7.5	1.509	0.841	41.719	1.151	0.228	47.770
8	7	8.5	1.039	0.667	48.805	0.758	0.199	55.501
8	7	9.5	0.686	0.545	56.466	0.474	0.177	63.850
8	7	10.5	0.431	0.458	64.855	0.280	0.159	72.959
8	7	11.5	0.254	0.393	73.942	0.153	0.146	82.778
8	7	12.5	0.138	0.344	83.736	0.075	0.134	93.302
8	7	13.5	0.066	0.305	94.235	0.031	0.125	104.517
8	7	14.5	0.026	0.275	105.425	0.009	0.118	116.401
8	7	15.5	0.007	0.251	117.286	0.001	0.111	128.922

Table C.I - Continued

v'	v''	J'	P_1	Q_1	R_1	P_2	Q_2	R_2
9	8	0.5	0.000	0.000	0.000	26.762	17.452	0.000
9	8	1.5	14.619	30.798	0.000	20.344	3.741	21.698
9	8	2.5	14.927	12.881	19.580	16.314	1.769	30.272
9	8	3.5	13.368	6.961	29.839	13.317	1.099	37.472
9	8	4.5	11.548	4.310	37.915	10.949	0.784	44.608
9	8	5.5	9.823	2.912	45.480	9.031	0.605	52.047
9	8	6.5	8.286	2.093	53.122	7.462	0.491	59.934
9	8	7.5	6.955	1.577	61.096	6.173	0.412	68.342
9	8	8.5	5.820	1.234	69.528	5.114	0.354	77.304
9	8	9.5	4.874	0.995	78.434	4.239	0.310	86.781
9	8	10.5	4.058	0.821	87.936	3.521	0.275	96.892
9	8	11.5	3.390	0.692	98.016	2.943	0.247	107.564
9	8	12.5	2.846	0.594	108.651	2.477	0.224	118.753
9	8	13.5	2.404	0.518	119.800	2.102	0.205	130.404
9	8	14.5	2.047	0.457	131.409	1.801	0.189	142.451
9	8	15.5	1.758	0.408	143.414	1.559	0.175	154.818

Table C.II: Einstein Coefficients (sec^{-1}) for $\Delta v=2$ Transitions

v'	v''	J'	P_1	Q_1	R_1	P_2	Q_2	R_2
2	0	0.5	0.000	0.000	0.000	9.311	4.590	0.000
2	0	1.5	5.905	7.946	0.000	8.641	1.026	4.247
2	0	2.5	7.186	3.228	3.468	8.470	0.506	4.940
2	0	3.5	7.704	1.692	4.495	8.454	0.323	5.120
2	0	4.5	7.996	1.017	4.858	8.498	0.232	5.122
2	0	5.5	8.200	0.668	4.959	8.567	0.179	5.040
2	0	6.5	8.360	0.468	4.932	8.645	0.143	4.910
2	0	7.5	8.494	0.343	4.835	8.725	0.117	4.750
2	0	8.5	8.611	0.261	4.697	8.803	0.099	4.571
2	0	9.5	8.707	0.205	4.524	8.869	0.084	4.372
2	0	10.5	8.798	0.164	4.341	8.936	0.072	4.170
2	0	11.5	8.878	0.135	4.146	8.996	0.063	3.963
2	0	12.5	8.947	0.112	3.944	9.048	0.055	3.752
2	0	13.5	9.007	0.095	3.736	9.091	0.049	3.539
2	0	14.5	9.056	0.081	3.525	9.126	0.044	3.325
2	0	15.5	9.095	0.070	3.313	9.151	0.039	3.111
3	1	0.5	0.000	0.000	0.000	26.456	13.021	0.000
3	1	1.5	16.742	22.592	0.000	24.531	2.891	12.070
3	1	2.5	20.367	9.197	9.827	24.024	1.416	14.027
3	1	3.5	21.823	4.827	12.733	23.955	0.900	14.522
3	1	4.5	22.638	2.903	13.753	24.055	0.646	14.510
3	1	5.5	23.198	1.907	14.025	24.224	0.496	14.256
3	1	6.5	23.629	1.333	13.933	24.417	0.396	13.864
3	1	7.5	23.984	0.977	13.638	24.612	0.325	13.385
3	1	8.5	24.283	0.742	13.221	24.795	0.272	12.847
3	1	9.5	24.546	0.581	12.729	24.970	0.232	12.275
3	1	10.5	24.764	0.465	12.179	25.115	0.199	11.669
3	1	11.5	24.946	0.380	11.592	25.235	0.173	11.042
3	1	12.5	25.094	0.316	10.980	25.329	0.152	10.402
3	1	13.5	25.209	0.266	10.350	25.395	0.134	9.753
3	1	14.5	25.292	0.226	9.710	25.432	0.119	9.102
3	1	15.5	25.344	0.195	9.065	25.442	0.107	8.451
4	2	0.5	0.000	0.000	0.000	48.139	23.617	0.000
4	2	1.5	30.419	41.064	0.000	44.658	5.211	21.891
4	2	2.5	37.037	16.757	17.762	43.757	2.537	25.400
4	2	3.5	39.717	8.812	22.990	43.656	1.605	26.251
4	2	4.5	41.236	5.308	24.803	43.867	1.150	26.185
4	2	5.5	42.290	3.488	25.260	44.205	0.882	25.681
4	2	6.5	43.111	2.439	25.059	44.588	0.704	24.930
4	2	7.5	43.790	1.787	24.491	44.973	0.579	24.022
4	2	8.5	44.369	1.357	23.700	45.339	0.485	23.010
4	2	9.5	44.892	1.062	22.806	45.688	0.413	21.959
4	2	10.5	45.308	0.850	21.768	45.968	0.355	20.815
4	2	11.5	45.657	0.693	20.663	46.200	0.309	19.636
4	2	12.5	45.940	0.575	19.512	46.380	0.271	18.433
4	2	13.5	46.160	0.484	18.329	46.507	0.239	17.215
4	2	14.5	46.317	0.412	17.128	46.577	0.212	15.992
4	2	15.5	46.412	0.354	15.917	46.590	0.190	14.770

Table C.II - Continued

v'	v''	J'	P_1	Q_1	R_1	P_2	Q_2	R_2
5	3	0.5	0.000	0.000	0.000	72.290	35.341	0.000
5	3	1.5	45.622	61.574	0.000	67.099	7.749	32.736
5	3	2.5	55.591	25.180	26.464	65.770	3.748	37.896
5	3	3.5	59.653	13.263	34.190	65.638	2.360	39.065
5	3	4.5	61.967	7.995	36.808	65.970	1.685	38.856
5	3	5.5	63.575	5.255	37.398	66.487	1.289	37.990
5	3	6.5	64.824	3.673	36.996	67.063	1.029	36.751
5	3	7.5	65.850	2.687	36.042	67.634	0.844	35.275
5	3	8.5	66.715	2.038	34.751	68.166	0.707	33.642
5	3	9.5	67.436	1.590	33.229	68.634	0.600	31.891
5	3	10.5	68.057	1.270	31.577	69.039	0.516	30.075
5	3	11.5	68.567	1.034	29.823	69.362	0.448	28.206
5	3	12.5	68.967	0.855	27.999	69.595	0.393	26.302
5	3	13.5	69.259	0.717	26.128	69.733	0.346	24.377
5	3	14.5	69.444	0.609	24.230	69.772	0.307	22.445
5	3	15.5	69.521	0.521	22.319	69.709	0.273	20.518
6	4	0.5	0.000	0.000	0.000	94.525	45.985	0.000
6	4	1.5	59.613	80.279	0.000	87.851	10.017	42.495
6	4	2.5	72.736	32.893	34.201	86.194	4.811	49.016
6	4	3.5	78.139	17.350	44.046	86.087	3.012	50.322
6	4	4.5	81.244	10.466	47.250	86.572	2.142	49.826
6	4	5.5	83.408	6.878	47.812	87.282	1.635	48.469
6	4	6.5	85.082	4.801	47.077	88.048	1.302	46.622
6	4	7.5	86.443	3.507	45.618	88.787	1.067	44.465
6	4	8.5	87.569	2.654	43.714	89.450	0.891	42.101
6	4	9.5	88.596	2.068	41.608	90.105	0.757	39.676
6	4	10.5	89.337	1.646	39.215	90.533	0.649	37.062
6	4	11.5	89.902	1.335	36.689	90.822	0.562	34.380
6	4	12.5	90.294	1.100	34.072	90.963	0.490	31.657
6	4	13.5	90.514	0.918	31.398	90.949	0.430	28.915
6	4	14.5	90.561	0.774	28.695	90.772	0.380	26.175
6	4	15.5	90.435	0.659	25.986	90.429	0.337	23.456
7	5	0.5	0.000	0.000	0.000	109.977	53.141	0.000
7	5	1.5	69.363	92.949	0.000	102.435	11.497	48.879
7	5	2.5	84.801	38.145	39.117	100.668	5.479	56.065
7	5	3.5	91.246	20.141	50.120	100.666	3.407	57.190
7	5	4.5	94.989	12.150	53.451	101.316	2.411	56.216
7	5	5.5	97.602	7.977	53.721	102.190	1.833	54.236
7	5	6.5	99.604	5.558	52.485	103.090	1.455	51.685
7	5	7.5	101.199	4.049	50.403	103.914	1.188	48.773
7	5	8.5	102.476	3.052	47.802	104.603	0.989	45.624
7	5	9.5	103.459	2.364	44.851	105.116	0.836	42.302
7	5	10.5	104.207	1.873	41.697	105.449	0.714	38.891
7	5	11.5	104.700	1.510	38.399	105.571	0.615	35.421
7	5	12.5	104.942	1.236	35.013	105.470	0.533	31.928
7	5	13.5	104.933	1.024	31.585	105.136	0.465	28.445
7	5	14.5	104.671	0.857	28.155	104.561	0.408	25.004
7	5	15.5	104.153	0.724	24.757	103.739	0.358	21.637
8	6	0.5	0.000	0.000	0.000	113.186	54.144	0.000
8	6	1.5	71.489	94.877	0.000	105.836	11.630	49.373
8	6	2.5	87.691	38.983	39.209	104.329	5.495	56.133
8	6	3.5	94.613	20.594	49.820	104.569	3.390	56.677
8	6	4.5	98.705	12.415	52.622	105.421	2.384	55.066
8	6	5.5	101.576	8.135	52.305	106.439	1.802	52.424
8	6	6.5	103.756	5.651	50.450	107.418	1.423	49.202
8	6	7.5	105.451	4.099	47.735	108.249	1.156	45.626
8	6	8.5	106.747	3.074	44.501	108.869	0.958	41.829
8	6	9.5	107.718	2.368	40.994	109.287	0.805	37.950
8	6	10.5	108.328	1.862	37.239	109.388	0.683	33.952
8	6	11.5	108.592	1.489	33.372	109.186	0.584	29.945
8	6	12.5	108.513	1.207	29.466	108.672	0.502	25.979
8	6	13.5	108.093	0.989	25.580	107.838	0.433	22.106
8	6	14.5	107.335	0.818	21.772	106.681	0.375	18.372
8	6	15.5	106.237	0.681	18.092	105.194	0.325	14.826

Table C.II - Continued

v'	v''	J'	P_1	Q_1	R_1	P_2	Q_2	R_2
9	7	0.5	0.000	0.000	0.000	101.441	47.786	0.000
9	7	1.5	64.303	83.877	0.000	95.487	10.184	42.922
9	7	2.5	79.309	34.483	33.706	94.627	4.764	48.106
9	7	3.5	85.957	18.209	42.240	95.236	2.912	47.771
9	7	4.5	89.996	10.957	43.906	96.299	2.029	45.523
9	7	5.5	92.856	7.155	42.829	97.416	1.522	42.375
9	7	6.5	95.005	4.945	40.411	98.396	1.193	38.739
9	7	7.5	96.618	3.562	37.259	99.137	0.961	34.834
9	7	8.5	97.770	2.649	33.688	99.580	0.789	30.794
9	7	9.5	98.394	2.017	29.861	99.668	0.656	26.707
9	7	10.5	98.787	1.569	25.987	99.478	0.550	22.683
9	7	11.5	98.737	1.238	22.101	98.887	0.464	18.767
9	7	12.5	98.252	0.989	18.295	97.896	0.393	15.034
9	7	13.5	97.344	0.796	14.651	96.514	0.334	11.553
9	7	14.5	96.028	0.646	11.247	94.748	0.283	8.396
9	7	15.5	94.316	0.526	8.154	92.601	0.240	5.630

Table C.III: Einstein Coefficients (sec^{-1}) for $\Delta v=3$ Transitions

v'	v''	J'	P_1	Q_1	R_1	P_2	Q_2	R_2
3	0	0.5	0.000	0.000	0.000	0.612	0.302	0.000
3	0	1.5	0.388	0.524	0.000	0.567	0.067	0.280
3	0	2.5	0.471	0.213	0.228	0.555	0.033	0.326
3	0	3.5	0.504	0.112	0.296	0.553	0.021	0.337
3	0	4.5	0.522	0.067	0.319	0.554	0.015	0.337
3	0	5.5	0.534	0.044	0.325	0.557	0.012	0.331
3	0	6.5	0.544	0.031	0.323	0.561	0.009	0.321
3	0	7.5	0.551	0.023	0.316	0.565	0.008	0.310
3	0	8.5	0.558	0.017	0.307	0.569	0.007	0.298
3	0	9.5	0.562	0.014	0.295	0.573	0.006	0.285
3	0	10.5	0.568	0.011	0.283	0.577	0.005	0.272
3	0	11.5	0.573	0.009	0.271	0.581	0.004	0.260
3	0	12.5	0.578	0.008	0.258	0.585	0.004	0.247
3	0	13.5	0.582	0.007	0.246	0.589	0.003	0.235
3	0	14.5	0.587	0.006	0.234	0.594	0.003	0.223
3	0	15.5	0.592	0.005	0.222	0.598	0.003	0.212
4	1	0.5	0.000	0.000	0.000	2.851	1.415	0.000
4	1	1.5	1.795	2.459	0.000	2.630	0.314	1.327
4	1	2.5	2.176	1.004	1.083	2.565	0.154	1.554
4	1	3.5	2.325	0.529	1.414	2.550	0.098	1.623
4	1	4.5	2.406	0.320	1.540	2.554	0.070	1.637
4	1	5.5	2.461	0.211	1.585	2.568	0.054	1.625
4	1	6.5	2.503	0.148	1.590	2.585	0.044	1.599
4	1	7.5	2.537	0.109	1.575	2.603	0.036	1.563
4	1	8.5	2.567	0.084	1.546	2.620	0.031	1.522
4	1	9.5	2.568	0.065	1.490	2.611	0.026	1.457
4	1	10.5	2.589	0.053	1.447	2.625	0.023	1.406
4	1	11.5	2.607	0.043	1.399	2.637	0.020	1.354
4	1	12.5	2.622	0.036	1.348	2.647	0.018	1.300
4	1	13.5	2.634	0.031	1.294	2.655	0.016	1.244
4	1	14.5	2.643	0.027	1.240	2.660	0.014	1.188
4	1	15.5	2.650	0.023	1.184	2.663	0.013	1.130
5	2	0.5	0.000	0.000	0.000	7.016	3.486	0.000
5	2	1.5	4.405	6.069	0.000	6.459	0.768	3.281
5	2	2.5	5.332	2.484	2.674	6.287	0.373	3.847
5	2	3.5	5.688	1.311	3.494	6.237	0.236	4.021
5	2	4.5	5.878	0.793	3.810	6.238	0.170	4.059
5	2	5.5	6.003	0.524	3.925	6.261	0.131	4.033
5	2	6.5	6.098	0.368	3.944	6.293	0.105	3.972
5	2	7.5	6.175	0.271	3.909	6.331	0.087	3.888
5	2	8.5	6.241	0.207	3.842	6.369	0.073	3.788
5	2	9.5	6.301	0.163	3.755	6.409	0.063	3.680
5	2	10.5	6.353	0.132	3.654	6.444	0.055	3.564
5	2	11.5	6.398	0.109	3.543	6.477	0.048	3.442
5	2	12.5	6.439	0.091	3.425	6.507	0.043	3.315
5	2	13.5	6.475	0.078	3.301	6.534	0.038	3.186
5	2	14.5	6.506	0.067	3.175	6.558	0.035	3.055
5	2	15.5	6.534	0.058	3.045	6.580	0.031	2.924

Table C.III - Continued

v'	v''	J'	P_1	Q_1	R_1	P_2	Q_2	R_2
6	3	0.5	0.000	0.000	0.000	13.863	6.886	0.000
6	3	1.5	8.681	12.015	0.000	12.750	1.508	6.505
6	3	2.5	10.504	4.931	5.291	12.402	0.729	7.636
6	3	3.5	11.204	2.610	6.925	12.299	0.460	7.992
6	3	4.5	11.580	1.582	7.564	12.300	0.330	8.082
6	3	5.5	11.831	1.046	7.809	12.349	0.254	8.048
6	3	6.5	12.023	0.737	7.864	12.421	0.204	7.944
6	3	7.5	12.184	0.543	7.815	12.505	0.169	7.796
6	3	8.5	12.326	0.416	7.703	12.594	0.143	7.620
6	3	9.5	12.451	0.328	7.550	12.682	0.123	7.424
6	3	10.5	12.570	0.265	7.369	12.773	0.107	7.214
6	3	11.5	12.681	0.219	7.171	12.864	0.094	6.994
6	3	12.5	12.788	0.184	6.959	12.955	0.084	6.768
6	3	13.5	12.890	0.156	6.739	13.046	0.075	6.538
6	3	14.5	12.991	0.135	6.513	13.138	0.068	6.305
6	3	15.5	13.090	0.118	6.284	13.232	0.062	6.071
7	4	0.5	0.000	0.000	0.000	24.583	12.206	0.000
7	4	1.5	15.356	21.342	0.000	22.590	2.657	11.567
7	4	2.5	18.576	8.785	9.392	21.961	1.277	13.593
7	4	3.5	19.813	4.662	12.309	21.775	0.802	14.244
7	4	4.5	20.482	2.832	13.465	21.779	0.573	14.427
7	4	5.5	20.935	1.877	13.926	21.874	0.441	14.391
7	4	6.5	21.289	1.323	14.053	22.017	0.355	14.233
7	4	7.5	21.592	0.977	13.995	22.185	0.294	14.000
7	4	8.5	21.864	0.749	13.825	22.368	0.249	13.716
7	4	9.5	22.199	0.593	13.658	22.644	0.216	13.474
7	4	10.5	22.444	0.480	13.372	22.843	0.188	13.133
7	4	11.5	22.679	0.396	13.052	23.044	0.166	12.772
7	4	12.5	22.909	0.333	12.706	23.248	0.148	12.397
7	4	13.5	23.133	0.284	12.343	23.454	0.133	12.011
7	4	14.5	23.356	0.245	11.964	23.662	0.121	11.615
7	4	15.5	23.577	0.214	11.575	23.874	0.110	11.212
8	5	0.5	0.000	0.000	0.000	40.292	19.985	0.000
8	5	1.5	25.110	35.019	0.000	37.000	4.323	18.988
8	5	2.5	30.369	14.453	15.385	35.950	2.063	22.322
8	5	3.5	32.391	7.689	20.174	35.634	1.288	23.401
8	5	4.5	33.486	4.680	22.084	35.635	0.918	23.712
8	5	5.5	34.233	3.106	22.858	35.792	0.705	23.663
8	5	6.5	34.820	2.191	23.081	36.031	0.567	23.413
8	5	7.5	35.326	1.618	22.999	36.315	0.470	23.037
8	5	8.5	35.783	1.240	22.732	36.623	0.398	22.574
8	5	9.5	36.185	0.977	22.331	36.922	0.343	22.036
8	5	10.5	36.592	0.790	21.855	37.251	0.299	21.461
8	5	11.5	36.982	0.651	21.315	37.580	0.264	20.845
8	5	12.5	37.357	0.546	20.725	37.909	0.235	20.195
8	5	13.5	37.720	0.465	20.094	38.235	0.211	19.516
8	5	14.5	38.073	0.401	19.429	38.559	0.191	18.809
8	5	15.5	38.419	0.349	18.733	38.881	0.173	18.076
9	6	0.5	0.000	0.000	0.000	60.248	29.811	0.000
9	6	1.5	37.478	52.345	0.000	55.320	6.405	28.344
9	6	2.5	45.336	21.653	22.895	53.737	3.033	33.277
9	6	3.5	48.359	11.542	29.991	53.250	1.881	34.830
9	6	4.5	49.997	7.035	32.788	53.237	1.334	35.227
9	6	5.5	51.109	4.670	33.883	53.453	1.021	35.076
9	6	6.5	51.977	3.293	34.146	53.785	0.818	34.613
9	6	7.5	52.712	2.430	33.942	54.173	0.677	33.949
9	6	8.5	53.364	1.858	33.447	54.586	0.572	33.142
9	6	9.5	53.844	1.458	32.663	54.924	0.491	32.149
9	6	10.5	54.426	1.175	31.843	55.366	0.428	31.156
9	6	11.5	54.959	0.966	30.906	55.783	0.376	30.080
9	6	12.5	55.443	0.807	29.871	56.168	0.334	28.931
9	6	13.5	55.880	0.684	28.751	56.521	0.298	27.713
9	6	14.5	56.273	0.586	27.556	56.838	0.268	26.429
9	6	15.5	56.622	0.507	26.291	57.118	0.242	25.082

Table C.IV: Einstein Coefficients (sec^{-1}) for $\Delta v=4$ Transitions

v'	v''	J'	P_1	Q_1	R_1	P_2	Q_2	R_2
4	0	0.5	0.000	0.000	0.000	0.065	0.032	0.000
4	0	1.5	0.041	0.055	0.000	0.060	0.007	0.029
4	0	2.5	0.049	0.022	0.023	0.058	0.003	0.033
4	0	3.5	0.052	0.011	0.030	0.057	0.002	0.033
4	0	4.5	0.054	0.007	0.031	0.056	0.001	0.032
4	0	5.5	0.054	0.004	0.031	0.055	0.001	0.030
4	0	6.5	0.054	0.003	0.029	0.054	0.001	0.028
4	0	7.5	0.053	0.002	0.027	0.053	0.001	0.025
4	0	8.5	0.052	0.002	0.025	0.051	0.001	0.022
4	0	9.5	0.042	0.001	0.016	0.041	0.000	0.014
4	0	10.5	0.041	0.001	0.014	0.040	0.000	0.012
4	0	11.5	0.039	0.001	0.011	0.038	0.000	0.009
4	0	12.5	0.038	0.000	0.009	0.037	0.000	0.007
4	0	13.5	0.036	0.000	0.007	0.035	0.000	0.006
4	0	14.5	0.035	0.000	0.006	0.034	0.000	0.004
4	0	15.5	0.034	0.000	0.004	0.032	0.000	0.003
5	1	0.5	0.000	0.000	0.000	0.257	0.125	0.000
5	1	1.5	0.162	0.218	0.000	0.239	0.028	0.116
5	1	2.5	0.199	0.089	0.093	0.236	0.014	0.134
5	1	3.5	0.214	0.047	0.121	0.236	0.009	0.138
5	1	4.5	0.223	0.029	0.130	0.239	0.006	0.137
5	1	5.5	0.230	0.019	0.132	0.242	0.005	0.134
5	1	6.5	0.236	0.013	0.131	0.246	0.004	0.130
5	1	7.5	0.241	0.010	0.127	0.249	0.003	0.125
5	1	8.5	0.246	0.008	0.123	0.253	0.003	0.120
5	1	9.5	0.252	0.006	0.120	0.258	0.002	0.116
5	1	10.5	0.256	0.005	0.115	0.261	0.002	0.110
5	1	11.5	0.259	0.004	0.109	0.264	0.002	0.104
5	1	12.5	0.262	0.003	0.104	0.266	0.002	0.099
5	1	13.5	0.265	0.003	0.098	0.268	0.002	0.093
5	1	14.5	0.267	0.003	0.092	0.270	0.001	0.087
5	1	15.5	0.269	0.002	0.087	0.271	0.001	0.082
6	2	0.5	0.000	0.000	0.000	0.841	0.414	0.000
6	2	1.5	0.529	0.722	0.000	0.779	0.091	0.387
6	2	2.5	0.644	0.296	0.313	0.762	0.044	0.450
6	2	3.5	0.690	0.157	0.407	0.760	0.028	0.467
6	2	4.5	0.717	0.095	0.441	0.764	0.020	0.468
6	2	5.5	0.736	0.063	0.451	0.770	0.016	0.462
6	2	6.5	0.751	0.044	0.450	0.778	0.013	0.451
6	2	7.5	0.763	0.033	0.443	0.785	0.010	0.438
6	2	8.5	0.775	0.025	0.432	0.793	0.009	0.424
6	2	9.5	0.786	0.020	0.420	0.801	0.008	0.409
6	2	10.5	0.794	0.016	0.406	0.807	0.007	0.393
6	2	11.5	0.802	0.013	0.390	0.813	0.006	0.376
6	2	12.5	0.808	0.011	0.374	0.817	0.005	0.359
6	2	13.5	0.813	0.010	0.357	0.820	0.005	0.341
6	2	14.5	0.817	0.008	0.340	0.822	0.004	0.323
6	2	15.5	0.819	0.007	0.322	0.823	0.004	0.306
7	3	0.5	0.000	0.000	0.000	1.924	0.950	0.000
7	3	1.5	1.205	1.659	0.000	1.773	0.207	0.893
7	3	2.5	1.461	0.682	0.723	1.727	0.100	1.042
7	3	3.5	1.561	0.361	0.941	1.715	0.063	1.084
7	3	4.5	1.615	0.219	1.022	1.717	0.045	1.089
7	3	5.5	1.651	0.145	1.048	1.724	0.035	1.076
7	3	6.5	1.678	0.102	1.048	1.733	0.028	1.053
7	3	7.5	1.700	0.075	1.034	1.743	0.023	1.025
7	3	8.5	1.718	0.058	1.010	1.753	0.020	0.993
7	3	9.5	1.734	0.046	0.984	1.762	0.017	0.960
7	3	10.5	1.746	0.037	0.951	1.769	0.015	0.923
7	3	11.5	1.756	0.030	0.916	1.775	0.013	0.885
7	3	12.5	1.764	0.026	0.880	1.779	0.012	0.847
7	3	13.5	1.770	0.022	0.842	1.783	0.010	0.809
7	3	14.5	1.775	0.019	0.805	1.785	0.009	0.771
7	3	15.5	1.778	0.016	0.767	1.787	0.009	0.733

Table C.IV - Continued

v'	v''	J'	P_1	Q_1	R_1	P_2	Q_2	R_2
8	4	0.5	0.000	0.000	0.000	3.752	1.858	0.000
8	4	1.5	2.341	3.252	0.000	3.450	0.403	1.757
8	4	2.5	2.834	1.341	1.422	3.355	0.193	2.059
8	4	3.5	3.025	0.713	1.859	3.327	0.121	2.151
8	4	4.5	3.128	0.434	2.027	3.328	0.087	2.170
8	4	5.5	3.198	0.288	2.090	3.342	0.067	2.157
8	4	6.5	3.251	0.203	2.102	3.362	0.054	2.125
8	4	7.5	3.296	0.151	2.086	3.385	0.045	2.083
8	4	8.5	3.335	0.116	2.054	3.410	0.038	2.034
8	4	9.5	3.380	0.092	2.022	3.446	0.033	1.993
8	4	10.5	3.415	0.075	1.976	3.474	0.029	1.939
8	4	11.5	3.448	0.062	1.925	3.502	0.026	1.884
8	4	12.5	3.480	0.052	1.873	3.530	0.023	1.829
8	4	13.5	3.512	0.045	1.820	3.560	0.021	1.776
8	4	14.5	3.545	0.039	1.768	3.593	0.019	1.724
8	4	15.5	3.579	0.035	1.717	3.628	0.018	1.674
9	5	0.5	0.000	0.000	0.000	7.202	3.578	0.000
9	5	1.5	4.476	6.278	0.000	6.606	0.772	3.412
9	5	2.5	5.411	2.599	2.763	6.415	0.368	4.020
9	5	3.5	5.772	1.388	3.631	6.360	0.230	4.226
9	5	4.5	5.971	0.849	3.986	6.365	0.164	4.297
9	5	5.5	6.111	0.566	4.141	6.400	0.127	4.306
9	5	6.5	6.225	0.402	4.200	6.454	0.103	4.284
9	5	7.5	6.326	0.299	4.208	6.518	0.086	4.243
9	5	8.5	6.422	0.231	4.188	6.590	0.073	4.191
9	5	9.5	6.483	0.183	4.116	6.642	0.063	4.103
9	5	10.5	6.584	0.149	4.072	6.734	0.056	4.046
9	5	11.5	6.686	0.125	4.021	6.830	0.050	3.988
9	5	12.5	6.790	0.106	3.968	6.932	0.045	3.930
9	5	13.5	6.898	0.092	3.914	7.041	0.042	3.874
9	5	14.5	7.012	0.080	3.861	7.160	0.038	3.822
9	5	15.5	7.135	0.071	3.811	7.291	0.036	3.775

Table C.V: Einstein Coefficients (sec^{-1}) for $\Delta v=5$ Transitions

v'	v''	J'	P_1	Q_1	R_1	P_2	Q_2	R_2
5	0	0.5	0.000	0.000	0.000	0.031	0.016	0.000
5	0	1.5	0.020	0.027	0.000	0.028	0.003	0.014
5	0	2.5	0.023	0.011	0.012	0.027	0.002	0.017
5	0	3.5	0.025	0.006	0.015	0.026	0.001	0.017
5	0	4.5	0.025	0.003	0.016	0.026	0.001	0.017
5	0	5.5	0.025	0.002	0.016	0.025	0.001	0.016
5	0	6.5	0.024	0.001	0.015	0.024	0.000	0.015
5	0	7.5	0.023	0.001	0.014	0.023	0.000	0.013
5	0	8.5	0.022	0.001	0.013	0.022	0.000	0.012
5	0	9.5	0.022	0.001	0.012	0.020	0.000	0.010
5	0	10.5	0.020	0.000	0.010	0.018	0.000	0.009
5	0	11.5	0.018	0.000	0.008	0.016	0.000	0.007
5	0	12.5	0.016	0.000	0.007	0.014	0.000	0.005
5	0	13.5	0.014	0.000	0.005	0.012	0.000	0.003
5	0	14.5	0.012	0.000	0.003	0.010	0.000	0.002
5	0	15.5	0.010	0.000	0.002	0.008	0.000	0.001
6	1	0.5	0.000	0.000	0.000	0.036	0.017	0.000
6	1	1.5	0.023	0.030	0.000	0.034	0.004	0.015
6	1	2.5	0.028	0.012	0.012	0.034	0.002	0.017
6	1	3.5	0.031	0.006	0.015	0.034	0.001	0.017
6	1	4.5	0.032	0.004	0.016	0.035	0.001	0.016
6	1	5.5	0.033	0.003	0.015	0.035	0.001	0.015
6	1	6.5	0.034	0.002	0.015	0.035	0.000	0.014
6	1	7.5	0.035	0.001	0.013	0.036	0.000	0.013
6	1	8.5	0.035	0.001	0.012	0.036	0.000	0.011
6	1	9.5	0.036	0.001	0.011	0.036	0.000	0.010
6	1	10.5	0.036	0.001	0.010	0.036	0.000	0.009
6	1	11.5	0.036	0.000	0.008	0.037	0.000	0.007
6	1	12.5	0.036	0.000	0.007	0.037	0.000	0.006
6	1	13.5	0.036	0.000	0.006	0.037	0.000	0.005
6	1	14.5	0.037	0.000	0.005	0.037	0.000	0.004
6	1	15.5	0.037	0.000	0.004	0.037	0.000	0.003

Table C.V - Continued

v'	v''	J'	P_1	Q_1	R_1	P_2	Q_2	R_2
7	2	0.5	0.000	0.000	0.000	0.120	0.058	0.000
7	2	1.5	0.076	0.101	0.000	0.113	0.013	0.052
7	2	2.5	0.094	0.041	0.042	0.113	0.006	0.060
7	2	3.5	0.103	0.022	0.053	0.114	0.004	0.061
7	2	4.5	0.108	0.013	0.057	0.117	0.003	0.060
7	2	5.5	0.113	0.009	0.057	0.120	0.002	0.058
7	2	6.5	0.117	0.006	0.056	0.123	0.002	0.055
7	2	7.5	0.121	0.005	0.054	0.126	0.002	0.053
7	2	8.5	0.125	0.004	0.052	0.130	0.001	0.050
7	2	9.5	0.129	0.003	0.050	0.134	0.001	0.048
7	2	10.5	0.133	0.002	0.048	0.138	0.001	0.046
7	2	11.5	0.137	0.002	0.045	0.141	0.001	0.043
7	2	12.5	0.140	0.002	0.043	0.145	0.001	0.041
7	2	13.5	0.144	0.002	0.040	0.148	0.001	0.038
7	2	14.5	0.148	0.001	0.038	0.151	0.001	0.036
7	2	15.5	0.151	0.001	0.036	0.155	0.001	0.034
8	3	0.5	0.000	0.000	0.000	0.387	0.188	0.000
8	3	1.5	0.243	0.329	0.000	0.360	0.041	0.174
8	3	2.5	0.298	0.135	0.140	0.354	0.020	0.201
8	3	3.5	0.321	0.072	0.180	0.355	0.012	0.207
8	3	4.5	0.335	0.044	0.194	0.359	0.009	0.206
8	3	5.5	0.346	0.029	0.197	0.364	0.007	0.201
8	3	6.5	0.355	0.021	0.195	0.369	0.006	0.195
8	3	7.5	0.363	0.015	0.190	0.375	0.005	0.187
8	3	8.5	0.370	0.012	0.184	0.380	0.004	0.179
8	3	9.5	0.367	0.009	0.171	0.376	0.003	0.164
8	3	10.5	0.372	0.007	0.162	0.379	0.003	0.155
8	3	11.5	0.377	0.006	0.154	0.382	0.003	0.146
8	3	12.5	0.380	0.005	0.144	0.384	0.002	0.136
8	3	13.5	0.382	0.004	0.135	0.385	0.002	0.126
8	3	14.5	0.384	0.004	0.125	0.386	0.002	0.116
8	3	15.5	0.384	0.003	0.116	0.385	0.002	0.107
9	4	0.5	0.000	0.000	0.000	0.800	0.391	0.000
9	4	1.5	0.501	0.685	0.000	0.741	0.084	0.365
9	4	2.5	0.610	0.282	0.292	0.724	0.040	0.422
9	4	3.5	0.654	0.150	0.378	0.721	0.025	0.434
9	4	4.5	0.679	0.091	0.406	0.724	0.018	0.431
9	4	5.5	0.696	0.060	0.412	0.729	0.014	0.421
9	4	6.5	0.709	0.043	0.408	0.734	0.011	0.407
9	4	7.5	0.720	0.031	0.397	0.739	0.009	0.390
9	4	8.5	0.728	0.024	0.383	0.742	0.008	0.372
9	4	9.5	0.742	0.019	0.370	0.756	0.007	0.359
9	4	10.5	0.749	0.015	0.354	0.761	0.006	0.341
9	4	11.5	0.755	0.013	0.337	0.764	0.005	0.322
9	4	12.5	0.759	0.011	0.319	0.766	0.005	0.304
9	4	13.5	0.761	0.009	0.301	0.766	0.004	0.285
9	4	14.5	0.762	0.008	0.283	0.765	0.004	0.267
9	4	15.5	0.762	0.007	0.265	0.763	0.003	0.249

ACKNOWLEDGMENTS

I am grateful to Dr. Walter J. Stevens and Dr. Morris Krauss for their cooperation in supplying the theoretical dipole moment functions, and their patience during the performance of these calculations. I wish to thank Dr. Paul Julienne for the use of his excellent computer program which was used to calculate the vibrational wavefunctions and the matrix elements required in this study. I am grateful to Dr. Randall E. Murphy for his encouragement and cooperation in supplying unpublished experimental data on the OH transitions. The calculations were supported in part by funds from the Air Force Cambridge Research Laboratories under the sponsorship of Dr. R. E. Murphy and Dr. A. T. Stair, Jr.

RECEIVED: January 28, 1974

REFERENCES

1. D. R. BATES AND M. NICOLET, *J. Geophys. Res.* **55**, 301 (1950).
2. A. B. MEINEL, *Astrophys. J.* **111**, 555 (1950); **112**, 120 (1950).

3. L. WALLACE, *J. Atmos. Sci.* **19**, 1 (1962).
4. V. I. KRASSOVSKY, N. N. SHEFOV, AND V. I. YARIN, *J. Atmos. Terr. Phys.* **21**, 46 (1961).
5. D. GARVIN, H. P. BROIDA, AND H. J. KOSTKOWSKI, *J. Chem. Phys.* **32**, 880 (1960).
6. P. E. CHARTERS, R. G. MACDONALD, AND J. C. POLANYI, *Appl. Optics* **10**, 1747 (1971).
7. A. B. CALLEAR AND H. E. VAN DEN BERGH, *Chem. Phys. Lett.* **8**, 17 (1971).
8. E. VIETZKE, H. I. SCHIFF, AND K. H. WELGE, *Chem. Phys. Lett.* **12**, 429 (1971).
9. G. J. KVIFTE, *Planet. Space Sci.* **5**, 153 (1971); **15**, 1515 (1967).
10. W. J. STEVENS, G. DAS, A. C. WAHL, D. NEUMANN, AND M. KRAUSS, *J. Chem. Phys.*, to be published.
11. R. E. MURPHY, *J. Chem. Phys.* **54**, 4852 (1971).
12. A. F. FERGUSON AND D. PARKINSON, *Planet. Space Sci.* **11**, 149 (1963).
13. D. L. ALBRITTON, private communication.
14. F. H. MIES, manuscript in preparation for submission to *J. Mol. Spectrosc.*
15. E. HILL AND J. H. VANVLECK, *Phys. Rev.* **32**, 250 (1928).
16. R. HERMAN AND R. F. WALLIS, *J. Chem. Phys.* **23**, 637 (1955); see also R. HERMAN, R. W. ROTHERY, AND R. J. RUBIN, *J. Mol. Spectrosc.* **2**, 369 (1958); AND J. K. CASHION, *J. Chem. Phys.* **41**, 3988 (1964).
17. See Appendix C, and data in Ref. (*14*).
18. M. E. ROSE, "Elementary Theory of Angular Momentum," Wiley, New York, 1957.
19. F. H. MIES, *Phys. Rev.* **7A**, 942, 957 (1973).
20. P. JULIENNE AND M. KRAUSS, "Molecules in the Galactic Environment," (M. A. Gordan and L. E. Snyder, Eds.), p. 353, Wiley, New York, 1973.
21. R. K. HINKLEY, J. A. HALL, T. E. H. WALKER AND W. G. RICHARDS, *J. Phys.* **B5**, 204 (1972).
22. W. KOLOS AND L. WOLNIEWICZ, *J. Chem. Phys.* **41**, 3663 (1964); **43**, 2429 (1965); **45**, 509 (1966); **51**, 1417 (1969).
23. R. GORDON, *J. Chem. Phys.* **51**, 14 (1969).
24. G. HERZBERG, "Spectra of Diatomic Molecules," 2nd ed., p. 232, Van Nostrand, Princeton, New Jersey, 1950.
25. E. A. MOORE AND W. G. RICHARDS, *Physica Scripta* **3**, 223 (1971).
26. T. E. H. WALKER AND W. G. RICHARDS, *Faraday Soc. Sympos.* **2**, 64 (1968); *Phys. Rev.* **177**, 100 (1969).
27. P. JULIENNE, *J. Mol. Spectrosc.* **48**, 508 (1973).
28. W. S. BENEDICT, E. K. PLYLER, AND C. J. HUMPHREYS, *J. Chem. Phys.* **21**, 398 (1953).
29. W. S. BENEDICT AND E. K. PLYLER, "Energy Transfer in Hot Gases," p. 57, National Bureau of Standards Circular 523, U.S. Govt. Printing Office, Washington, D.C., 1954.
30. A. W. HARRISON AND D. J. W. KENDALL, *J. Geophys. Res.* **78**, 4697 (1973).
31. A. E. POTTER, JR., R. N. COLTHARP, AND S. D. WORLEY, *J. Chem. Phys.* **54**, 992 (1971).
32. J. D'INCAN, C. EFFANTIN, AND F. ROUX, *J. Quant. Spectrosc. Radiat. Trans.* **11**, 1215 (1971).
33. W. H. HENNEKER AND H. E. POPKIE, *J. Chem. Phys.* **54**, 1763 (1971).
34. A. MESSIAH, "Quantum Mechanics," Chap. VII, Wiley, New York, 1965.
35. K. R. GERMAN, T. H. BERGEMAN, E. M. WEINSTOCK, AND R. N. ZARE, *J. Chem. Phys.* **58**, 4304 (1973).